UNCLASSIFIED

AD 437 260

DEFENSE DOCUMENTATION CENTER

FOR

SCIENTIFIC AND TECHNICAL INFORMATION

CAMERON STATION. ALEXANDRIA. VIRGINIA

UNCLASSIFIED

64-12

LINDE COMPANY
DIVISION OF UNION CARBIDE CORPORATION
SPEEDWAY LABORATORIES
INDIANAPOLIS, INDIANA

LINDE DIVISION
Union Carbide Corporation
Speedway Laboratories
Indianapolis, Indiana

Final Report

Fabrication and Deformation

of Tungsten Single Crystals

Part I

"Effect of Billet Rolling Plane

and Rolling Direction on the

Recrystallization Temperature of Sheet

from Tungsten Single Crystals"

Prepared by: A. C. Walters, R. G. Rudness, M. Stern
Linde Division, Union Carbide Corporation, Prime Contractor

Part II

"Recrystallization of Worked Single

Crystals of Tungsten"

Prepared by: W. G. Reuter, L. Raymond, E. L. Harmon
Aeronutronic Division, Ford Motor Corporation, Subcontractor

Prepared for: Contract NOw-61-0671-c

The Materials Branch,

Bureau of Naval Weapons

August 28, 1963

TABLE OF CONTENTS

TABLE OF CONTENTS (Cont'd.)

LIST OF FIGURES

LIST OF FIGURES (Cont'd.)

LIST OF TABLES

SUMMARY

The sheet rolled from the [011](100) oriented tungsten single crystal billet had an increasingly superior recrystallization temperature over the [100](001), [100](011)., and [011](0̄11) orientations at all reductions in thickness tested in the order given. This substantiates the premise on which the study was begun that the recrystallization temperature is dependent on the initial billet rolling plane-rolling direction orientations. This dependence seems related to the slip systems available for deformation and the values of shear stress from the compressive rolling stress resolved on these slip planes. A special "easy deformation mode" is shown as possibly existing in those rolling orientations having the highest recrystallization temperatures in which a slip direction and rolling direction are coplanar with a force direction acting on a favorably oriented slip plane to give a high resolved shear stress and cause deformation to occur in the direction of rolling. In addition, the varying rates of strain hardening, tensile strengths, recrystallization initiation, and recrystallized grain size are displayed as a function of billet orientation. A single crystal billet scale-up, as-rolled and rolled-recrystallized sheet texture study, and alloy program are recommended.

INTRODUCTION

A dependence of recrystallization kinetics on rolling plane-rolling direction when rolled as a single crystal in a study of iron-3% silicon[1] prompted the idea that this dependence might exist for other b.c.c. materials when rolled to sheet.

The interest in affecting both the warm working properties for easy deformation and the recrystallization temperature for improved high temperature properties in tungsten prompted the idea of a study to roll single crystals of tungsten with definite oriented rolling planes and rolling directions and observe the effect of orientation on recrystallization temperature. It was felt that the warm rolling temperatures could also be reduced below those usually used for tungsten because of the single crystal structure vs. the polycrystalline structure usually used.

In an attempt to determine why certain rolling plane-rolling direction combinations had better recrystallization kinetics than others as shown in the silicon-iron study mentioned above, simple deformation models were constructed. These consisted of the unit cubes as they would be oriented in the billet rolling plane-rolling direction combinations of interest, the slip systems operative, the rolling forces, and the relative levels of the resolved shear stress caused by the rolling forces available to initiate slip in the model.

From this model reasons were advanced as to why some orientations might deform more easily than others thereby retaining less energy from the deformation in the matrix capable of triggering recrystallization. This ease of deformation should then yield a wrought structure with a lower strength and

- 1 -

better ductility at a given reduction than an orientation which did not have an easy mode of deformation.

I.   PROPOSAL OF A SIMPLIFIED THEORETICAL DEFORMATION MODEL

The model used in this study was concerned with the relative magnitudes of resolved shear stress acting on the components of the slip systems as induced in a rolling operation of an oriented single crystal with a body-center cubic lattice. These resolved shear stress magnitudes along with the relationship of the associated slip directions to the direction of force and rolling direction were noted for the five rolling plane-rolling direction combinations used in this study: the [011](100), [100](001) [100](011), [011](0$\bar{1}$1), and [111](1$\bar{1}$0). The first three rolling direction-rolling plane combinations considered were those used in the silicon-iron study[1] ranked in their experimentally determined order of increasing rate of recrystallization kinetics. The last two are combinations which supplement the list of low Miller's index rolling combinations of interest which could be obtained with [100], [110], and [111] seeds.

A.   Review of Published Work on Slip Systems in Tungsten

Plastic deformation occurs by slip in certain crystallographic directions, usually the direction of most dense packing, and on certain crystallographic planes, usually the planes of most dense packing with the greatest interplanar spacing containing a slip direction. For a body-center cubic lattice, the structure of tungsten, most investigators agree the directions of slip are the $\langle 111 \rangle$.[2,3,4] The planes responsible for slip, however, are in dispute. Early work cited the {112} as the slip planes.[2] Later work brought out the possibility of temperature dependence on the operative slip system, with the {112} planes responsible at working temperatures below 650°C, the {110} planes responsible from 650°C to 2300°C, and the {123} planes above 2300°C.[3] This latter work was performed on metallic sodium single crystals, however, and the tungsten crystals were studied and evaluated only at low temperatures. The sodium results were expressed as a ratio of working temperature over the absolute melting point of the material and the results extrapolated for tungsten. Recent work on tungsten single crystals predicts the slip planes at 25°C and above to be both the {110} and the {112} mixed.[4] This work was felt to be most valid. Therefore, resolved shear stress in the rolling models was calculated for both the {112} $\langle 111 \rangle$ and {110} $\langle 111 \rangle$ slip systems. No interactions between members of the same system or the other systems were considered for the sake of model simplicity and the lack of pertinent equations. The components of both slip systems are shown in Figures 1 and 2.

B.   Resolved Shear Stress in Model

The formula used to calculate resolved shear stress on the slip planes in the direction of slip for the rolling model was:
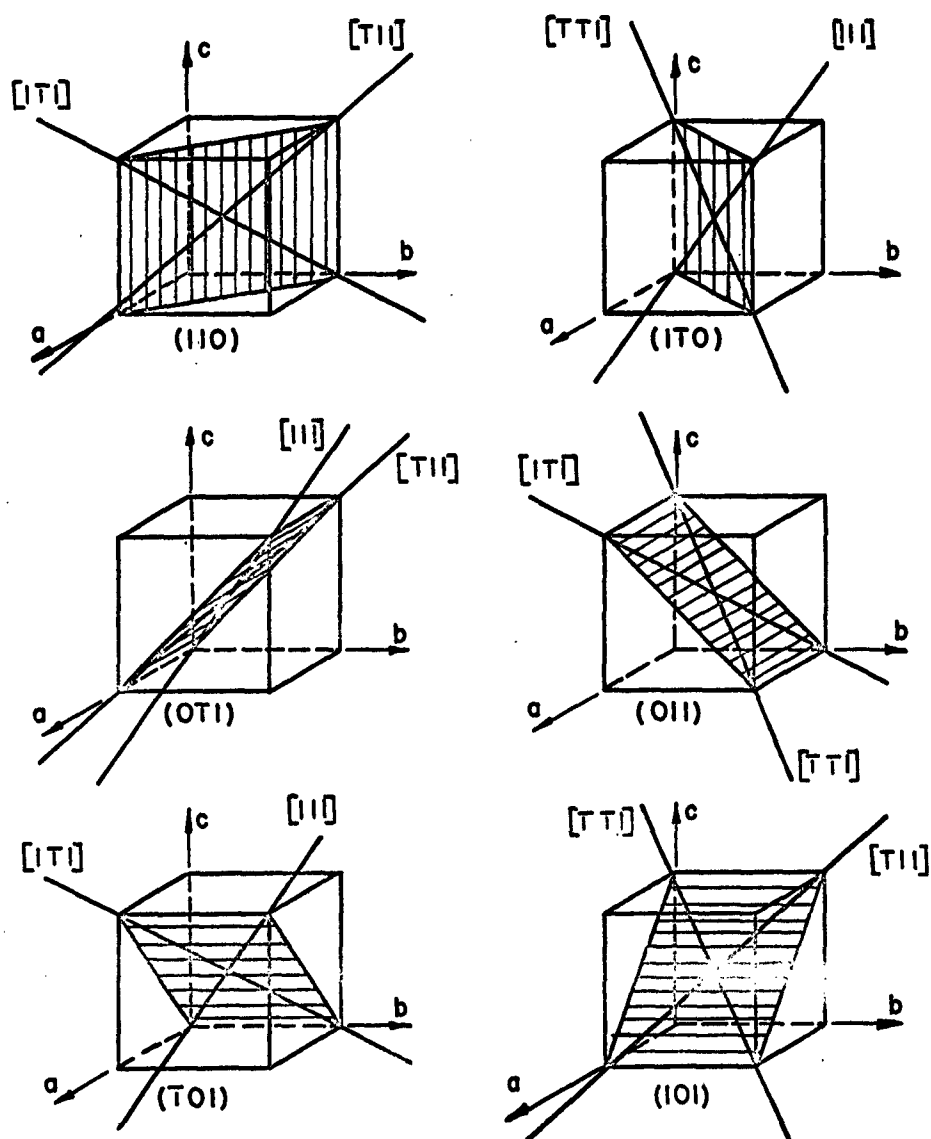
FIGURE I

{110} ⟨11⟩ SLIP SYSTEM FOR CUBICS

[hkl] SLIP DIRECTIONS SHOWN BY HEAVY LINES

(hkl) SLIP PLANES SHOWN BY CROSS-HATCHED REGIONS
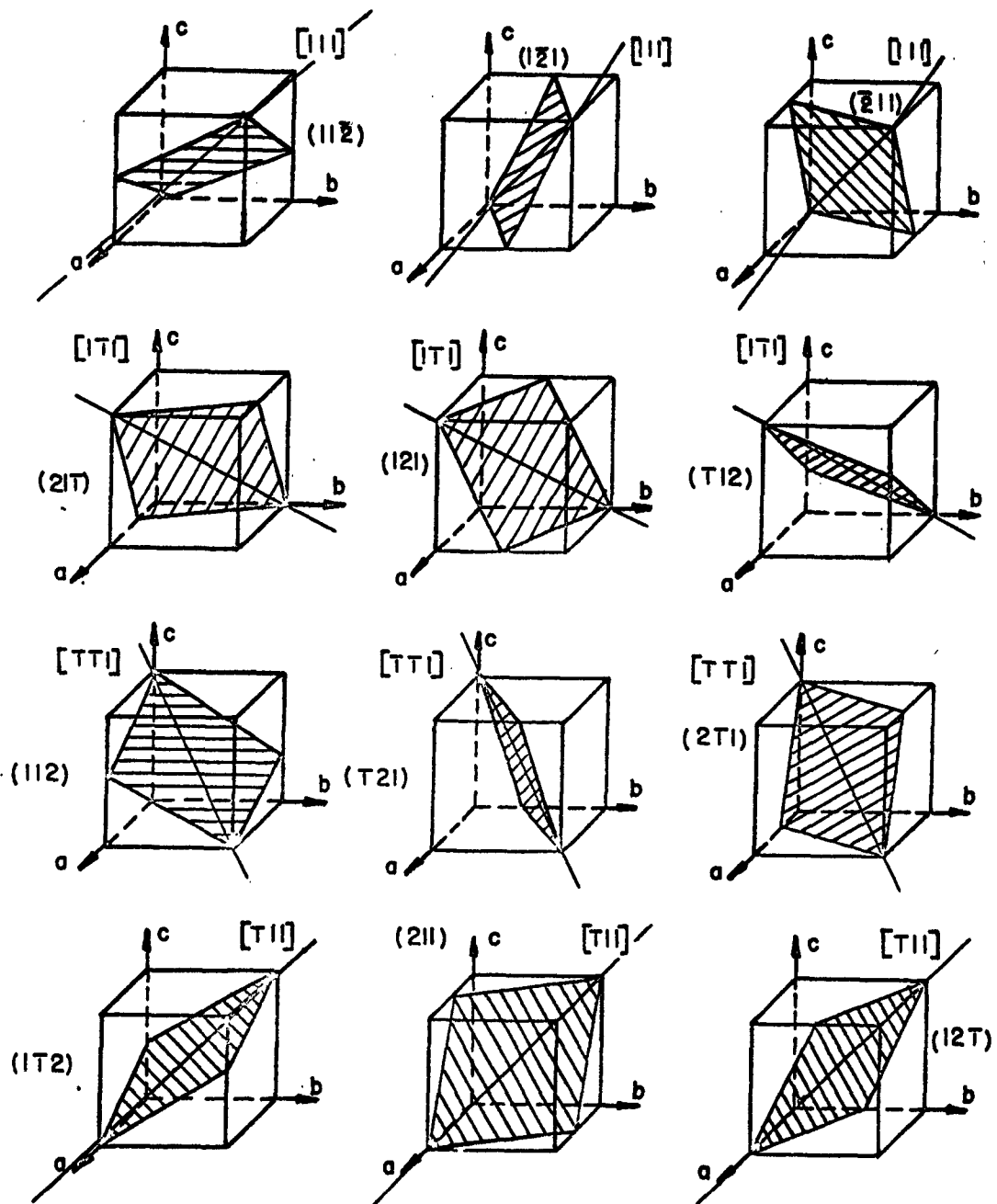
FIGURE 2

{112} ⟨111⟩ SLIP SYSTEM FOR CUBICS

[hkl] SLIP DIRECTIONS SHOWN BY HEAVY LINES

(hkl) SLIP PLANES SHOWN BY CROSS—HATCHED REGIONS

$$\Upsilon = \frac{F}{A} \cdot \cos \phi \cdot \cos \lambda \qquad (1)$$

As shown on the cubic model in Figure 3, (F) is the compressive force due to rolling and is assumed to be perpendicular to the rolling plane, uniform in magnitude, and constant in direction along the arc of contact between the rolls and the workpiece. These are not in serious error if the reduction is small and the roll radius is large compared to the thickness.[5] The area (A) on which the force is acting is assumed to be constant as the model does not increase in width but only in length with no volume change. The quantity (F/A) can then be considered to be equal to the engineering stress (σ_c) sigma compressive. The angles phi and lambda refer to angular measure between the force direction and the normal to the slip plane, and between the force direction and the slip direction, respectively, measured in degrees.

The angles between the force direction (F) and slip plane normal, and the force direction (F) and the slip direction, were calculated by assigning Miller Indices to the directions, which are perpendicular to planes having the same Miller Indices for the cubic lattices.

$$\cos \phi \quad \text{or} \cos \lambda \quad = \frac{h_1 h_2 + k_1 k_2 + l_1 l_2}{\sqrt{(h_1{}^2 + k_1{}^2 + l_1{}^2)(h_1{}^2 + k_1{}^2 + l_1{}^2)}} \qquad (2)$$

where $[h_1 k_1 l_1]$ and $[h_2 k_2 l_2]$ are the Miller Indices of the directions. Calculating these values for $\cos \phi$ and $\cos \lambda$ and substituting them in equation (1) yields a value for (Υ) the resolved shear stress stated in terms of the unknown constant (σ_c).

C. Calculation of Resolved Shear Stress

The calculations were performed for the twelve components of the $\{110\} \langle 111 \rangle$ and the twelve components of the $\{112\} \langle 111 \rangle$ slip systems in each of the five rolling direction-rolling plane combinations depicted in Figure 4. These were shown as the orientation a unit cell would possess in the lattice when observed in the direction of rolling.

The results of the calculations for all components of both slip systems for the five rolling combinations were listed in Table I and understood to be stated in terms of (σ_c) in each case. High values of (Υ) indicated an active slip plane-slip direction on which slip was likely to occur. A value of zero for (Υ) indicated no slip was possible due to an unfavorably oriented slip plane, slip direction, or both.

D. Discussion of Calculations

From Table I, the calculated values of the shear stress resolved on the available slip systems for each of the five rolling combinations

- 5 -

F

λ   φ

SLIP PLANE
NORMAL

SLIP
PLANE

CROSS
SECTION
AREA

SLIP
DIRECTION

F
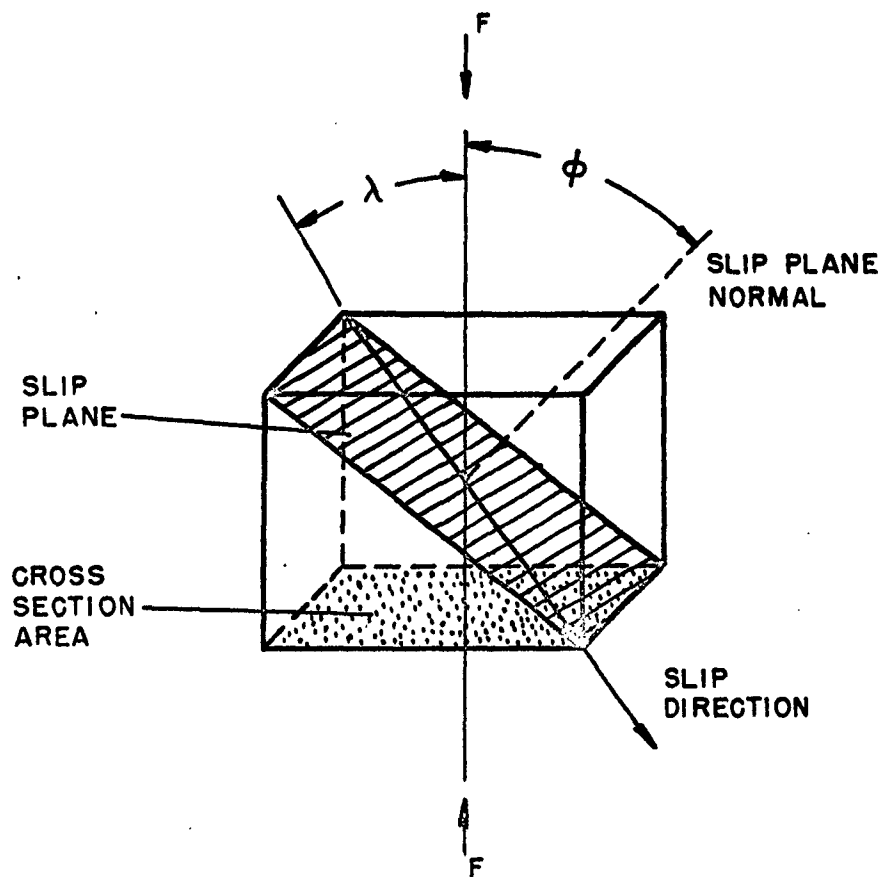
FIGURE 3

SCHEMATIC   DEFINING   SLIP   PLANE   NORMAL   AND
SLIP   DIRECTION   ANGLES   FOR   FORMULA   OF
RESOLVED   SHEAR   STRESS.

$$T = \sigma_c \cos \phi \cos \lambda$$
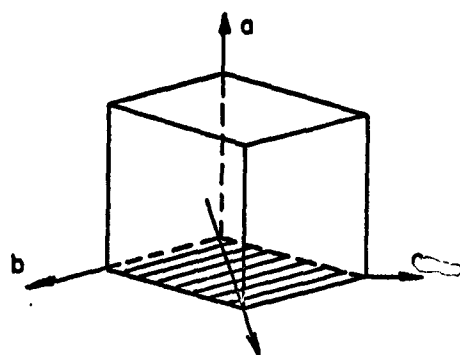
(100) [0̄11] ROLLING PLANE-
ROLLING DIRECTION
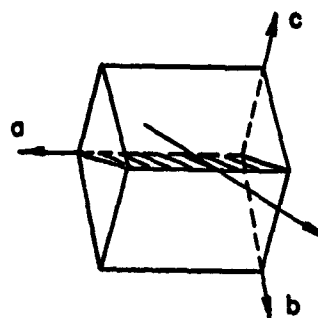
(0̄11) [0̄11] ROLLING PLANE-
ROLLING DIRECTION
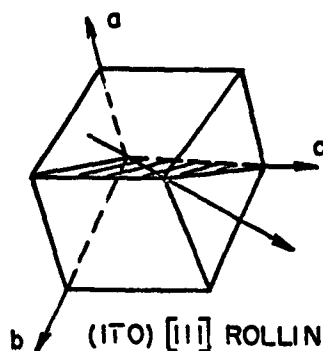
(1̄10) [111] ROLLING PLANE-
ROLLING DIRECTION
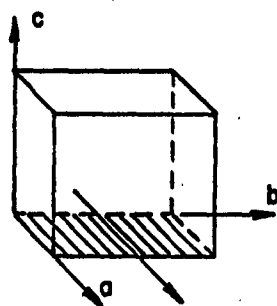
(001) [1̄00] ROLLING PLANE-
ROLLING DIRECTION
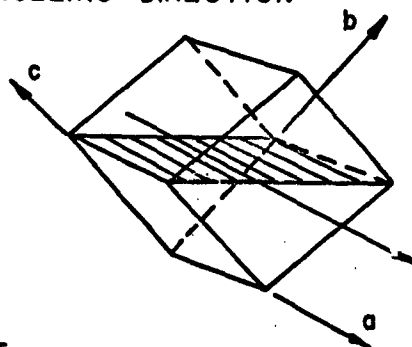
(011) [1̄00] ROLLING PLANE-
ROLLING DIRECTION

FIGURE 4

SCHEMATIC OF CUBE

ORIENTATIONS FOR ROLLING PLANE- ROLLING

DIRECTION GEOMETRY

TABLE I

RESULTS OF CALCULATION OF RESOLVED SHEAR STRESS (τ)

IN TERMS OF THE COMPRESSIVE STRESS (σ)

Slip System	Rolling Direction - Rolling Plane Combination				
	[011](100)	[011](0Ī1)	[111](1Ī0)	[100](001)	[100](011)
[111](11Ī)	0.236	0	0	0.473	0.236
[111](1Ī1)	0.236	0	0	0.236	0.236
[111](Ī11)	0.473	0	0	0.236	0.473
[1Ī1](21Ī)	0.473	0.473	0.236	0.236	0
[1Ī1](121)	0.236	0.236	0.236	0.236	0
[1Ī1](Ī12)	0.236	0.236	0.473	0.473	0
[ĪĪ1](112)	0.236	0.236	0	0.473	0
[ĪĪ1](Ī21)	0.236	0.236	0	0.236	0
[ĪĪ1](2Ī1)	0.473	0.473	0	0.236	0
[Ī11](1Ī2)	0.236	0	0.473	0.473	0.236
[Ī11](211)	0.473	0	0.236	0.236	0.473
[Ī11](12Ī)	0.236	0	0.236	0.236	0.236
[1Ī1](110)	0.41	0.41	0	0	0
[Ī11](110)	0.41	0	0	0	0.41
[111](1Ī0)	0.41	0	0	0	0.41
[ĪĪ1](1Ī0)	0.41	0.41	0	0	0
[Ī11](0Ī1)	0	0	0.41	0.41	0
[111](0Ī1)	0	0	0	0.41	0
[1Ī1](011)	0	0	0.41	0.41	0
[ĪĪ1](011)	0	0	0	0.41	0
[1Ī1](Ī01)	0.41	0.41	0.41	0.41	0
[111](Ī01)	0.41	0	0	0.41	0.41
[ĪĪ1](101)	0.41	0.41	0	0.41	0
[Ī11](101)	0.41	0	0.41	0.41	0.41

Summary	[011](100)	[011](0Ī1)	[111](1Ī0)	[100](001)	[100](011)
Active Slip Systems High Value	12	6	6	12	6
Low Value	8	4	4	8	4
Inactive Slip Systems	4	14	14	4	14

shows the [011](100) and [100](001) combinations contain the greatest number of active components of the $\{112\} \langle 111 \rangle$ and $\{110\} \langle 111 \rangle$ slip systems. These two rolling combinations had slower recrystallization kinetics than the other combinations evaluated in the iron-3% silicon study.[1]

A closer inspection of the deformation models of the two combinations shows a possible explanation as to why the [011](100) had slower recrystallization kinetics than the [100](001) rolling plane-rolling direction fabricated crystal.

The [011](100) rolling plane-rolling direction combination has two $\langle 111 \rangle$ slip directions, common to the $\{112\}$ and $[110]$ slip planes. Both of these slip directions lie in an imaginary plane formed by the direction of applied force and the rolling direction as shown in the bottom figure and the inset in Figure 5. The [100](001) combination shown in the top of Figure 5 has no $\langle 111 \rangle$ directions coplanar with the direction of application of force and rolling directions.

This arrangement of forces and slip directions might be the explanation for the results shown experimentally in the silicon-iron study that when a crystal is rolled so that slip takes place on planes with a high resolved shear stress in a direction coplanar with the force and the rolling directions, then deformation occurs with substantially less strain hardening as evidenced by the slower recrystallization kinetics. This seemed to be substantiated in the gross effect for the oriented tungsten single crystal billets used for this study as shown by a higher recrystallization temperature for the [011](100) billet.

II. MATERIAL PREPARATION

A. Seed Growth

Efforts to grow tungsten single crystals via the arc-Verneuil process with closely aligned boule axis and desired crystallographic rolling direction were begun by machining unalloyed tungsten single crystals grown in previous work to smooth cylinders 3/8-inch diameter by 2 inches in length with flat, parallel ends perpendicular to the axis of the cylinder. The crystallographic orientations necessary were those coinciding with the rolling directions to be used in the program; the [111], [011], and [100] directions.

Three smooth tungsten crystal cylinders nominally of the above orientations were electrolytically polished in a sodium hydroxide solution on one face to remove the distorted material from machining and grinding. Laue Back-Reflection photographs were taken and the results used to make the necessary corrections on the crystals in order to machine a cylinder from the seed stock axially coincident with the desired growth direction. The seeds were then repolished and checked by the Laue Back-Reflection technique for deviation from desired crystallographic orientation.
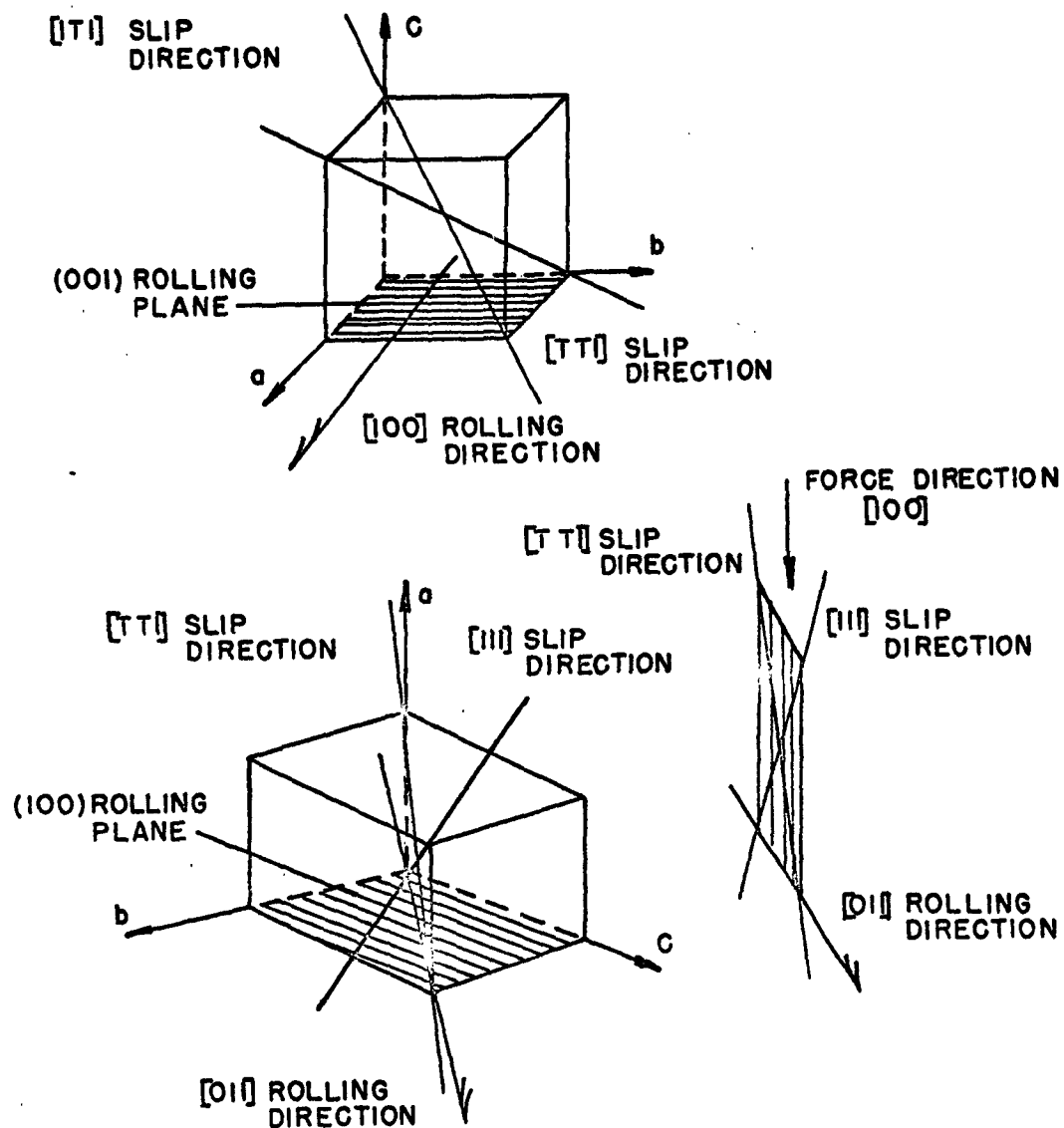
FIGURE 5

TOP- (001) [100] ROLLING COMBINATION

BOTTOM — (100) [011] ROLLING COMBINATION

INSET— SHOWS THE TWO SLIP DIRECTIONS LYING IN

PLANE WITH FORCE DIRECTION AND ROLLING

DIRECTION FOR (100) [011] ROLLING COMBINATION

B. Crystal Growth of Cylindrical Boules

Twenty tungsten crystals were grown from commercial quality tungsten powder using the Arc-Verneuil technique. The tungsten seeds described above were used to grow eight [011], eight [100], and four [111] crystals, with the designated crystallographic direction parallel to the cylindrical axis of the crystal. The nominal size of the as-grown crystals was 7/16 inches in diameter and 8 inches long.

The twenty crystals were selected from a larger group on the basis of X-ray structural and orientation analysis described below as representing a best effort to produce four crystals of each of the five rolling plane-rolling direction combinations listed in Table II.

Ten of the crystals are shown in Figure 6 as-grown minus the seed and a 1-1/2-inch sample length taken from the final growth end. The labels on the crystals designate both the data book number and the growth direction. The scribe line seen on several of the crystals was used to locate the desired rolling plane for machining the rolling billet once orientation had been determined on the sample length.

C. Slab Crystal Growth

The Arc-Verneuil technique was used to grow a slab-shaped tungsten crystal 1-1/2-inches by 3/8-inch by 12 inches long shown in Figure 7. In this growth trial the rectangular growth interface was obtained by traversing the hot plasma source reciprocally across the interface, rather than hold it stationary as was done to grow the cylindrical crystals. The slab crystal was not a single crystal at the final growth end but contained several areas comprising 25% of the cross-sectional area of crystallites unrelated in orientation to the major portion of the crystal. For this reason, rolling was not attempted on this slab crystal.

D. Analytical Methods for Crystal Selection

A 1-1/2-inch long sample was cut from the cap, or final growth, end of each crystal using a water-cooled cut-off wheel, the cylinder end surface ground with a silicon carbide wheel normal to the growth axis, and electrolytically etched in a 5% NaOH solution. A 1/2-inch section of this sample that contained the ground and etched face was cropped and used for a Back-Reflection Laue orientation determination and Schulz-Wei Zone-Reflection analysis for crystalline perfection. Depending on the deviation from the desired crystallographic growth direction and the extent of the internal grain-boundary misorientations, the crystals were found acceptable for or rejected from the program.

The remaining inch of the sample length was carefully cleaved and chips were taken from interior portions of the crystal. The large chips were analyzed conductometrically for carbon and oxygen, while the

TABLE II

TUNGSTEN CRYSTAL LIST

Crystal Number	Rolling Direction	Rolling Plane	Final Dimensions		
			Thickness (in.)	Width (in.)	Length (in.)
1616-12	[011]	(100)	0.234	0.360	6
1616-14	[011]	(100)	0.236	0.360	6
1616-16	[100]	(001)	0.235	0.297	3
1616-26	[011]	(0̄11)	0.147	0.340	6
1616-30	[100]	(001)	0.133	0.180	3.3
			0.140	0.211	2.3
1616-34	[011]	(0̄11)	0.159	0.353	5.8
1616-38	[100]	(011)	0.164	0.302	2
1616-40	[111]	(1̄10)	0.241	0.364	6
1616-42	[111]	(1̄10)	0.239	0.359	6
1616-44	[100]	(011)	0.239	0.361	6
1616-46	[111]	(1̄10)	0.251	0.375	5.9
1616-48	[111]	(1̄10)	0.250	0.375	6
1616-50	[011]	(0̄11)	0.250	0.377	5.9
1616-57	[011]	(0̄11)	0.250	0.376	6
1616-65	[100]	(001)	0.251	0.377	6
1616-70	[100]	(011)	0.252	0.377	6
1616-73	[100]	(011)	0.251	0.375	6.2
1616-74	[100]	(001)	0.251	0.375	5.9
1690-9	[011]	(100)	0.250	0.368	6
1690-12	[011]	(100)	0.249	0.367	6
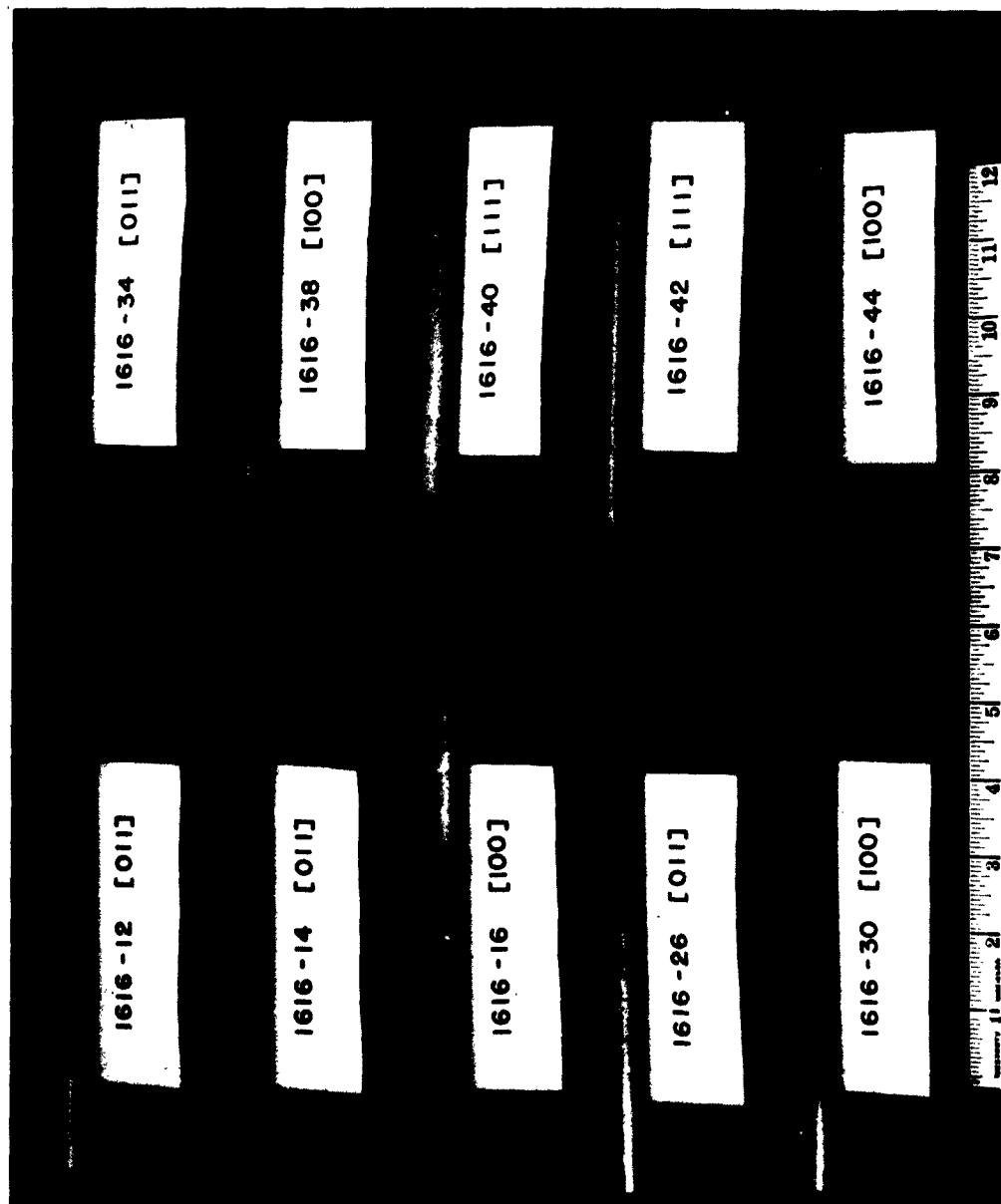
Tungsten crystals as-grown minus seed and sample length. Tag indicates growth direction. Scribe line used for machining rolling plane. Reduced 0.45 for reproduction.
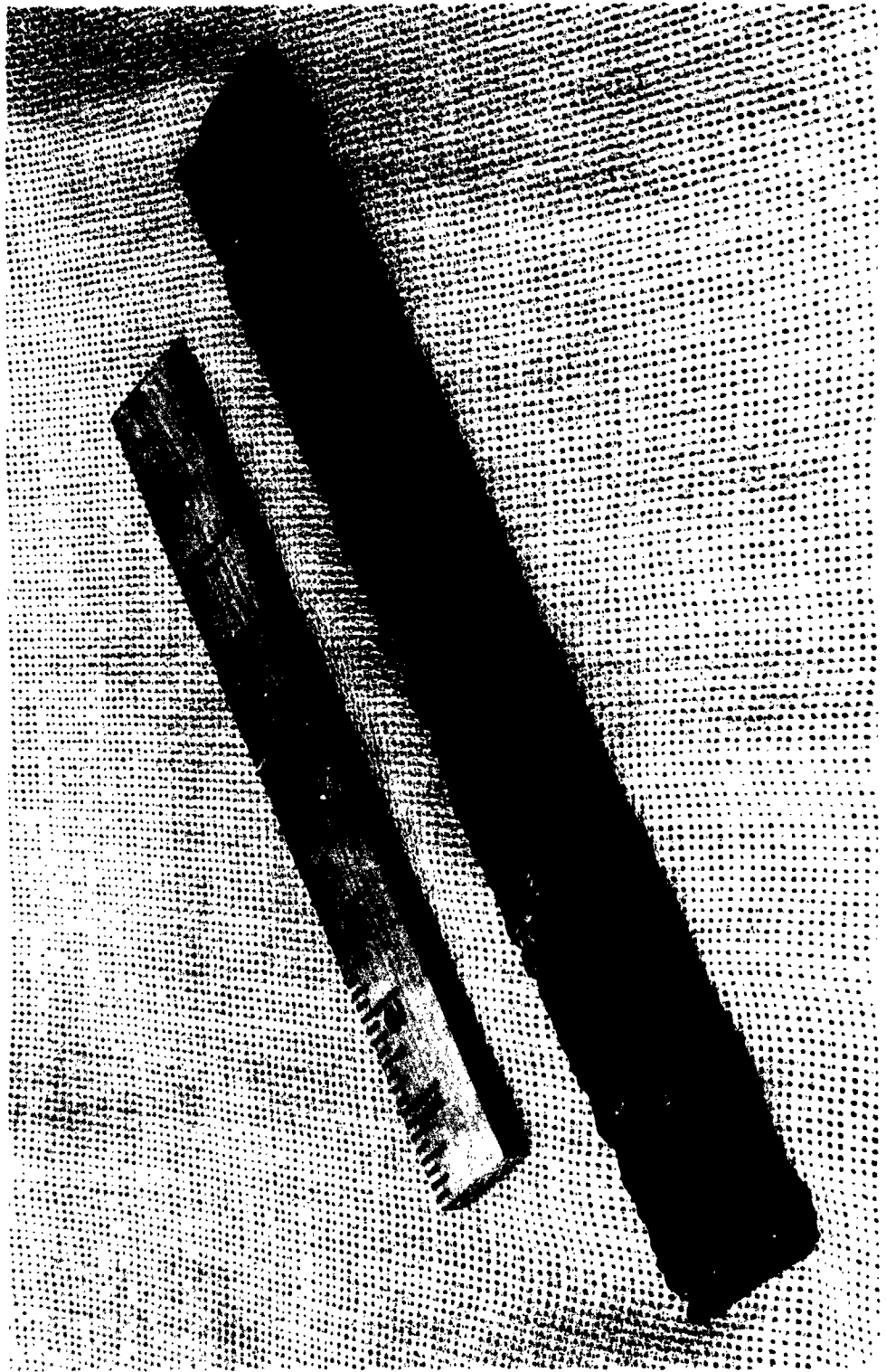
Tungsten crystal as-grown in a slab or billet shape. Initial exploratory try.

smaller chips were pulverized in a Platner Diamond mortar between platinum sheets and used to determine the levels of metallic impurities present in the tungsten crystals by spectrochemical analysis. The Harvey Semi-quantitative method[6] was used and the data presented as exponential quantities. No nitrogen or hydrogen analyses were run since past experience has shown the content of each to be less than 1 p.p.m. The results of the chemical analysis are shown in Table III.

E. Billet Orientation and Fabrication

Flats were machined on the crystals to correspond to the rolling plane desired using the longitudinal scribe line on each crystal. Rotation of this scribe line around the cylindrical axis of the crystal prescribed by the results of the Back-Reflection Laue shots brought the plane to the horizontal position as viewed along the axis of rotation.

In the first attempt at crystal billet fabrication, the crystals were clamped between parallel vise jaws to hold them during grinding of the rolling planes. The crystal-holding fixture caused failures in three of the [100] crystals, as well as fine, hairline surface cracks in several others. Ostensibly, the clamping pressure from the vise jaws in contact with the slightly irregular crystal surface during the grinding of the initial flats induced bending moments in the crystals resulting in fractures and surface cracks. The fractures in the crystals appeared to have taken place along the $\{100\}$ planes, the accepted cleavage planes for tungsten.[4] A view of the fractured surface and some of the resulting hairline cracks along the $\{100\}$ planes are shown in Figures 8, 9, and 10.

An improved technique found to prevent fracture and surface cracking during machining was to orient the crystals as before and mount them on steel plates with DeKhotinsky cement thus supporting the uneven crystal surface at every point as well as firmly holding the crystal rigid for grinding. The crystal and plate were placed on the magnetic chuck of a surface grinder and ground along the desired rolling plane until a 1/4-inch wide flat was obtained along the length of the crystal. The crystal was demounted, the opposite side exposed, remounted on the steel plate, and ground on the opposite side yielding a crystal with two parallel flats. This crystal could then be clamped in a parallel jaw vise for the remainder of the machining operation with no danger of inducing bending moments and causing fracture and surface cracking. A group of ten billets fabricated in this way is shown in Figure 11.

F. Surface Preparation Before Rolling

The machined crystal billets were chemically etched in a 70 vol. pct. HF - 30 vol. pct. HNO_3 neat solution and 0.005 to 0.007 inches dissolved from each face of the billet to remove the distorted surface layers caused by grinding. It was felt these distorted surfaces, if not removed,

TABLE III

CHEMICAL ANALYSIS OF TUNGSTEN CRYSTAL BILLETS

Crystal Number	Rolling Direction	Rolling Plane	C ppm	O ppm	Weight Per Cent										
					Al	Co	Cu	Cr	Fe	Mg	Mn	Mo	Ni	Si	Sn
1616-12	[011]	(100)	3	3					10^{-3}			10^{-2}		10^{-3}	
1616-14	[011]	(100)	3	4				10^{-3}	10^{-3}			10^{-2}		10^{-3}	
1616-16	[100]	(001)	3	4					10^{-3}			10^{-2}	10^{-3}	10^{-3}	
1616-26	[011]	(0$\bar{1}$1)	5	3					10^{-3}			10^{-2}		10^{-2}	
1616-30	[100]	(001)	5	4				10^{-3}	10^{-3}			10^{-2}	10^{-3}	10^{-3}	
1616-34	[011]	(0$\bar{1}$1)	3	4					10^{-3}			10^{-2}			
1616-38	[100]	(011)	3	4					10^{-3}			10^{-2}			
1616-40	[111]	(1$\bar{1}$0)	4	3					10^{-3}			10^{-2}			
1616-42	[111]	(1$\bar{1}$0)	3	4	10^{-3}			10^{-3}	10^{-3}		10^{-3}	10^{-3}		10^{-3}	
1616-44	[100]	(011)	4	3					10^{-3}		10^{-3}	10^{-2}			
1616-46	[111]	(1$\bar{1}$0)	6	4	10^{-3}			10^{-3}	10^{-3}			10^{-2}			
1616-48	[111]	(1$\bar{1}$0)	3	11	10^{-3}			10^{-3}	10^{-3}			10^{-2}			
1616-50	[011]	(0$\bar{1}$1)	5	3						10^{-4}					
1616-57	[011]	(0$\bar{1}$1)	4	3	10^{-3}	---Not detected---		10^{-3}	10^{-3}			10^{-2}			
1616-65	[100]	(001)	2	4					10^{-3}						
1616-70	[100]	(011)	3	3			10^{-4}		10^{-3}						
1616-73	[100]	(011)	2	5		---Not detected---									
1616-74	[100]	(001)	4	3						10^{-4}		10^{-2}		10^{-3}	
1690-9	[011]	(100)	3	5						10^{-4}					
1690-12	[011]	(100)	3	5											

Nominal Lower Limit of Detectability - $8 \cdot 10^{-3}$ $3 \cdot 10^{-3}$ $3 \cdot 10^{-4}$ $2 \cdot 10^{-3}$ $6 \cdot 10^{-3}$ $3 \cdot 10^{-4}$ $3 \cdot 10^{-3}$ $2 \cdot 10^{-2}$ $3 \cdot 10^{-3}$ $3 \cdot 10^{-3}$ $9 \cdot 10^{-3}$

NOTE: Interstitial Analysis Quantitative, Accuracy - $\pm 40\%$

Metallic Analysis Semi-Quantitative, Accuracy - 10^{-2} = 0.01-0.1%

10^{-3} = 0.001-0.01%
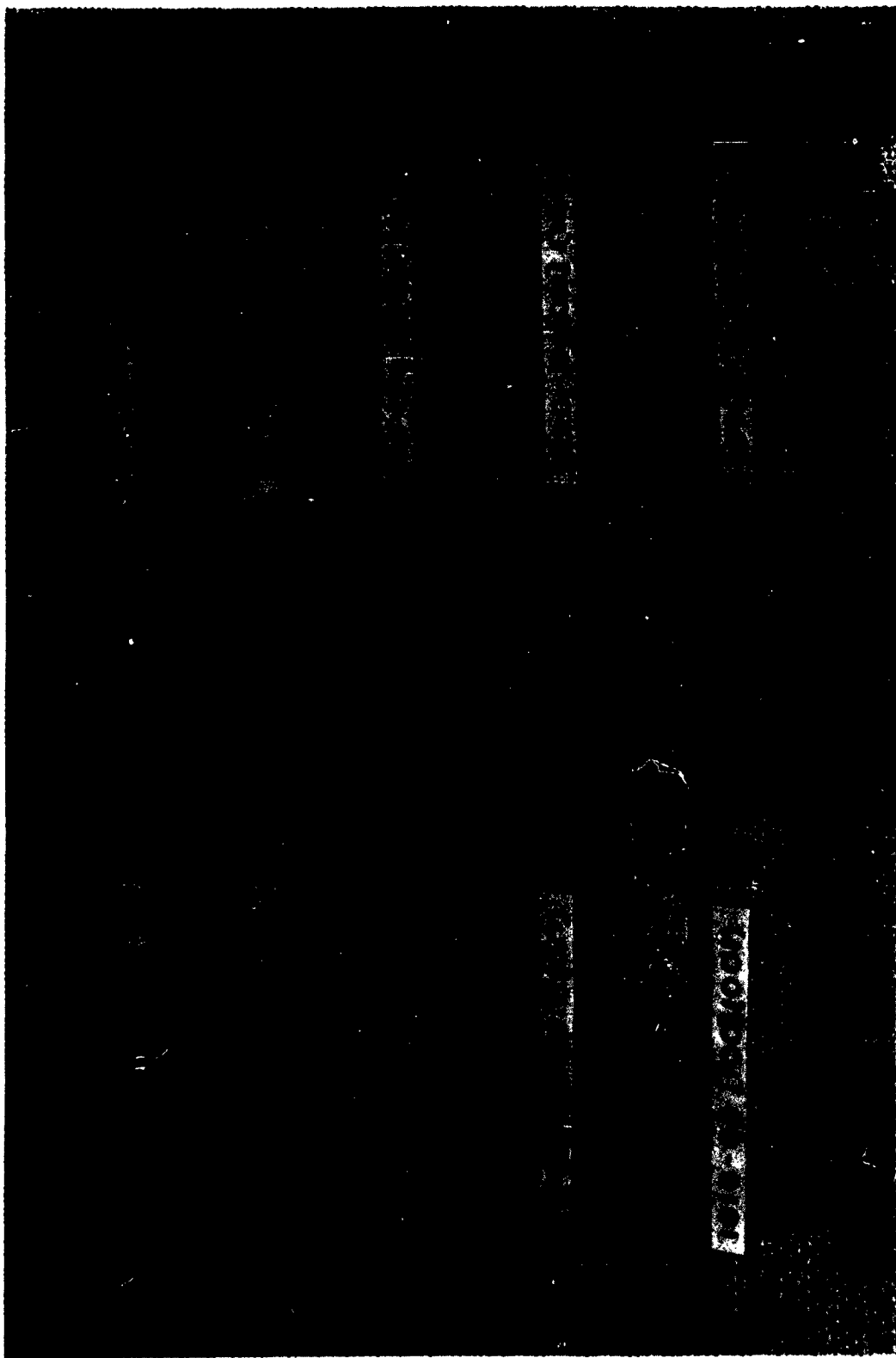
10^{-4} = 0.0001-0.001%

Transverse cross-section showing fracture of crystal along (100) plane. Mag. 4X.

As-machined billet showing transverse surface cracks normal to [100], viewed on (011) rolling plane. Mag. 2.25X.

Etched billet showing acid widened cracks normal to [100], viewed on (001) rolling plane. Etchant HF-HNO$_3$. Mag. 1X.

Tungsten crystals after machining and etching.

would interfere with the investigation by contributing sources for nucleating premature recrystallization during the initial heating to rolling temperature.

The HF-HNO_3 etch worked quickly and uniformly to produce a smooth, bright surface in most cases. In the exceptions, the (100) planes, the revelation of substructure was felt to be unavoidable and not detrimental to the rolling operation. It was deemed more important that the distorted surface had been removed.

G. Final Orientation Analysis Before Rolling

A 1/2-inch sample was cropped from the cap, or final growth, end of all the crystal billets produced for the contract, surface-ground normal to the rolling direction, and electrolytically polished in 5% sodium-hydroxide solution. To determine the deviation of the longitudinal axis of the crystal billet from the desired rolling direction and the deviation of the normal to the billet rolling plane from the desired rolling plane normal, a second Back-Reflection Laue photograph was taken. A second Schulz-Wei photograph was taken of each of the samples to determine the number and magnitude of low-angle grain boundaries present in the final billet. One of these photographs is seen in Figure 12 in which the rectangular cross-section of the billet is oriented so that the rolling plane is horizontal. This billet cross-section shape was somewhat aberrated in the low-index diffraction patterns occupying the top-center position in all the films, but showed quite clearly in the high-index images lower on the films.

Most of the patterns of the crystal billets showed the presence of only a few low-angle boundaries; however, Figure 13 shows a mosaic structure denoting several crystallites making up the entire crystal billet and misoriented by small angles.

The degree of misorientation can be qualitatively appreciated, but not quantitatively predicted, by casual observation of these photographs. Apparently, gross separations between crystallites can be overestimated as to degree of misorientation because of the vertical position of the image on the film. A more complete discussion of the quantitative aspects of the method is found elsewhere.[7]

The X-ray results of billet orientation deviation and internal grain boundary misorientation for all crystals produced for the contract are shown in Table IV.

III. ROLLING

A. Recommended Procedures

The tungsten single crystal billets were rolled at the facilities of the sub-contractor. The complete description, results, and discussion
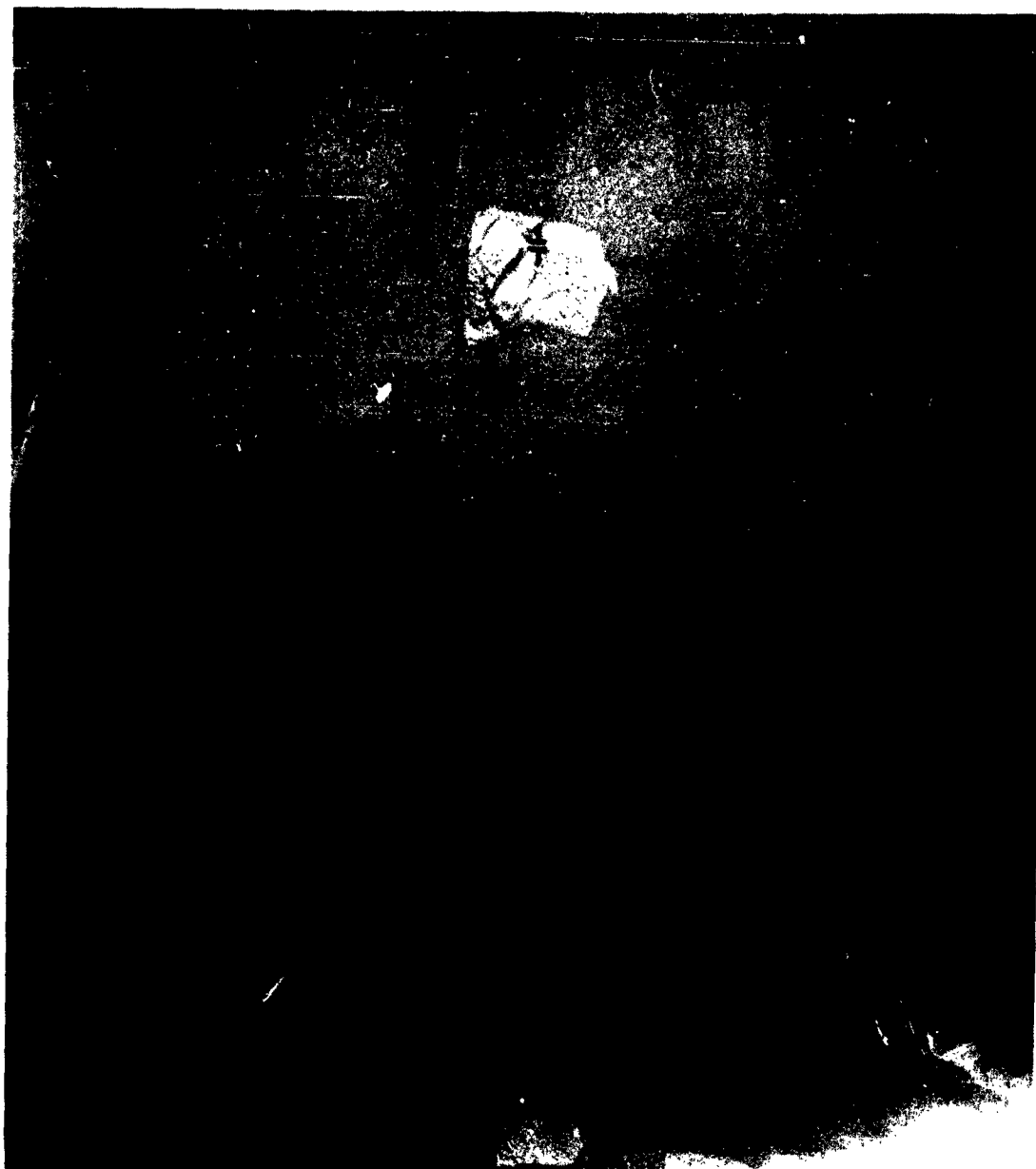
Schulz photo of 1616-26 [011] (0$\bar{1}$1) transverse cross-section.
[011] is perpendicular to page, (0$\bar{1}$1) normal lies along vertical
in page. Bracket shows 7' boundary on {110} zone-reflection.

Schulz photo of 1616-38 [100] (011) transverse cross-section.
[100] is perpendicular to page, (011) normal lies along vertical
in page. Bracket shows 49' boundary on {100} zone-reflection.

TABLE IV

X-RAY ANALYSIS RESULTS ON TUNGSTEN CRYSTAL BILLETS

Crystal Number	Rolling Direction	Rolling Plane	Deviation of Crystal Axis from Rolling Direction		Deviation of Rolling Plane Normal to Ground Flat	Maximum Low-Angle Grain Boundary
1616-12	[011]	(100)	1° →	3° →	1°	1°32'
1616-14	[011]	(100)	2° →	2° →	0°	1°2'
1616-16	[100]	(001)	1° ↓	3°	0°	53'
1616-26	[011]	(0T1)	4° ↓	4°	3°	7'
1616-30	[100]	(001)	1° ↓	3° →	2°	19'
1616-34	[011]	(0T1)	3° ↓	0°	4°	4°36'
1616-38	[100]	(011)	3° ↓	0°	1°	49'
1616-40	[100]	(011)	0°	0°	3°	31'
1616-42	[111]	(1T0)	5° ↓	5°	1°	33'
1616-44	[100]	(1T0)	1° ↓	1° ↗	3°	1°3'
1616-46	[111]	(011)	4° ↓	4° ↗	2°	1°
1616-48	[111]	(1T0)	4° ↓	3° ↗	1°	1°
1616-50	[011]	(1T0)	5° ↓	5° ↗	3°	1°
1616-57	[011]	(0T1)	1/2° →	1/2° ↓	5°	1°40'
1616-65	[100]	(001)	5° ↓	1° ↗	5°	15'
1616-70	[100]	(011)	2° ↓	1° ↗	3°	1°30'
1616-73	[100]	(011)	2° ↓	0° ↗	1°	1°
1616-74	[100]	(011)	4° →	3° ↗	7°	2°30'
1690-9	[011]	(001)	2° →	0° ↗	4°	30'
1690-12	[011]	(100)	1/2° ←	5° ←	6°	1°45'

of this work is found in the portion of the report submitted by the
sub-contractor. However, the rolling procedures used on the billets
for the author's phase of the contract work will be briefly outlined,
since the results of the rolling procedures on these billets must
necessarily affect the evaluation.

The schedule of rolling temperatures used after various cumu-
lative reductions in thickness and found to be successful is shown below:

Cumulative Reduction in Thickness	Temperature of Billet for Rolling
0 - 28%	950°C
28 - 53%	875°C
53 - 70%	800°C
70 - 87%	650°C
87 - 92%	600°C

In the rolling of these billets, the mean reduction per pass
was to be 10% and the billets were not to be reversed end for end between
passes since it was desired that slip should continually occur on the same
set of planes and in the same direction for each pass, giving a mode of
deformation with uniformity and lowest probability for storage of energy
in the matrix.

B. Initial Results

Five crystals were rolled in the first attempt:

Crystal Number	Rolling Direction	Rolling Plane
1616-14	[011]	(100)
1616-26	[011]	(0$\bar{1}$1)
1616-30	[100]	(001)
1616-40	[111]	(1$\bar{1}$0)
1616-44	[100]	(011)

A 60% reduction in thickness given Crystal 1616-14 [011](100) was
unintentionally accomplished in one pass at 950°C. Ten percent reductions
per pass were specified in all cases; however, in this case, a full size
crystal was passed through the rolls at a setting intended for a billet
of reduced size. This heavy first reduction was thought to be responsible
for a significant increase in width of the billet. The fact of some inter-
est was that the crystal could take a reduction of that magnitude at 950°C
and not fracture. This crystal rolling plane-rolling direction had the
geometry of greatest interest in the sheet study, since it was the [011](100)
iron-silicon single crystal which had the slowest recrystallization kinetics
determined in the work on which this program was based.[1]

Crystal 1616-26 [011](0$\bar{1}$1) fractured longitudinally on the (100) plane, the accepted cleavage plane for tungsten,[4] and is shown in Figure 14. The cause was felt to be that the 20% reduction attempted in one pass was too great for the operative slip systems to accommodate in this rolling direction-rolling plane combination. It will be remembered that the calculations of the resolved shear stress on the {112} ⟨111⟩ and {110} ⟨111⟩ slip systems for the [011](0$\bar{1}$1) rolling direction-rolling plane combination revealed a poor list of values for this particular rolling geometry. Of the twelve {112} ⟨111⟩ slip systems possible, six were inoperative, four had a stress acting on them that was less than one-quarter of the value of the applied compressive stress, and only two had stresses acting on them which were around one-half the applied compressive stress. Of the twelve {110} ⟨111⟩ slip systems, eight were inactive and four had a resolved shear stress acting on them around one-half the applied compressive stress.

This was one of the poorer rolling geometries of the group investigated, and the lack of slip systems could account for the failure. The stress on the fracture plane must have been greater than those resolved and acting on the available slip systems for the large reduction in thickness attempted.

Crystals 1616-40 [111](1$\bar{1}$0), shown in Figure 15, and 1616-44 [100](011), shown in Figures 16 and 17, did not roll straight but rolled in an arc lying in the plane of rolling. This was felt to be due to improper placement of the billets in the rolling fixture prior to pushing it into the rolls. Further rolling attempts on crystals of the [111](1$\bar{1}$0) rolling geometry, however, continued to be frustrated by a gross curve lying in the plane of rolling making any further reductions in thickness impossible. This rolling defect initially seemed caused by improper rolling procedures, however, a closer look revealed more interesting and plausible reasons for the behavior.

A review of the billet unit cube orientation when viewed in the direction of rolling showed a symmetrical arrangement of slip directions as can be seen in the top view of Figure 18. However, a view of the same billet unit cube from the top pointed out an asymmetry not noticed in the two-dimensional rolling direction view. A comparison of the orientation of the unit cube in a billet of the [100](001) and the [111](1$\bar{1}$0) rolling direction-rolling plane shows that an unfavorable anisotropy of possible slip directions existed prohibiting straight rolling of the [111](1$\bar{1}$0) orientation. Nonsymmetry of the [1$\bar{1}$1] and [$\bar{1}$11] slip directions with respect to the [111] direction when rolled on the (1$\bar{1}$0) plane seemed to be the cause. In the other four rolling geometries investigated, [011](100), [100](001), [100](011), and [011](0$\bar{1}$1), the ⟨111⟩ slip directions are symmetrical with respect to the rolling direction and the rolling plane as exemplified with the [100](001) orientation. Therefore, these rolling geometries when rolled correctly by entering the material into the rolls with the rolling direction normal to the axis of the rolls should produce straight sheet stock. However, if the material were fed into the rolls at some angle other than 90 degrees, or if the slip systems were asymmetrical

Crystal 1616-26 [011] (0$\bar{1}$1) shown fractured along (100) cleavage plane after an attempted 20% reduction in one pass. Note shape of two segments after splitting.
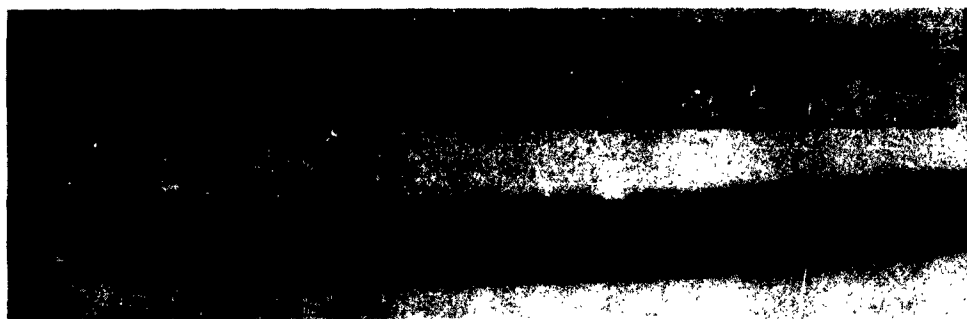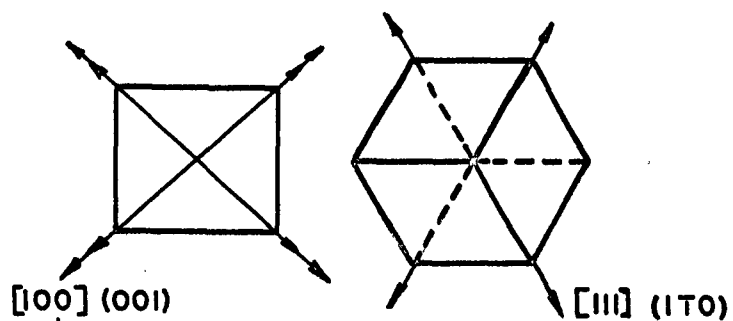

Crystal 1616-40 [111] (1$\bar{1}$0) shown formed in a curve lying in the plane of rolling after a 4% reduction in thickness.

Crystal 1616-44 [100] (011) shown formed in a curve lying in the plane of rolling after a 30% reduction in thickness in four passes.
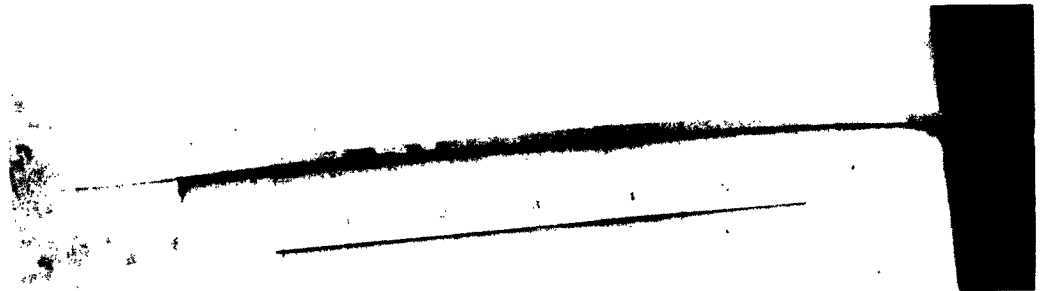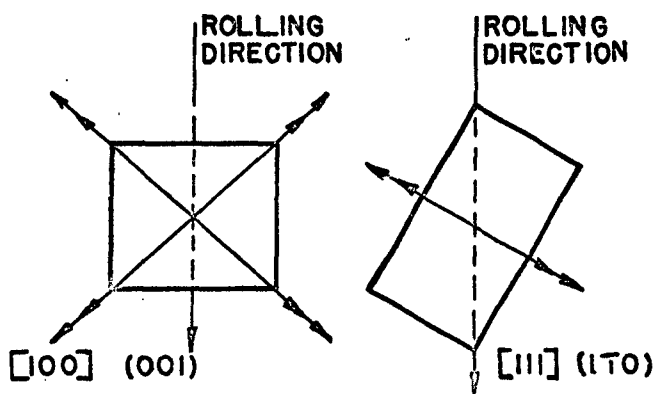

Crystal 1616-44 [100] (011) shown formed in a curve following the curvature of the rolls. 30% reduction in thickness in four passes.

DOUBLE HEADED ARROWS
REPRESENT TWO SUPER-
IMPOSED SLIP DIRECTIONS
WHICH WOULD BE RESOLVED
IN A 3-DIMENSIONAL VIEW.

[100] (001)   [111] (1̄10)

FRONT OR ROLLING DIRECTION VIEW

ROLLING   ROLLING
DIRECTION   DIRECTION

NOTE LACK OF SYMMETRY OF
SLIP DIRECTIONS ABOUT THE
ROLLING DIRECTION IN THE
TOP VIEW OF [111] (1̄10).

[100] (001)   [111] (1̄10)

TOP OR ROLLING PLANE VIEW

FIGURE 18

SCHEMATIC SHOWING THE ORIENATIONS OF THE UNIT CUBES IN BILLETS
OF THE [100] (001) AND [111] (1̄10) ROLLING GEOMETRY.

with respect to the rolling direction, then a net material transport
to one side of the billet might take place causing the billet to be
curved toward the side deficient in material. This curve would lie
in the plane of rolling as did those actually observed in the rolling.
Therefore, while correct rolling procedures prevented curving in the
four "symmetrical" orientations, the same procedures would not correct
the curving in the [111](1T0) rolling combination.

The rolling defect of gross curving on billets of the [111](1T0)
orientation was tested to see if it was lack of symmetry of the available
slip directions about the direction of rolling. A Laue Back-Reflection
X-ray shot of a [111](1T0) billet cross-section determined the unit cube
orientation and a prediction made as to the direction curling would take.
The crystal was rolled so that the unit cube was in the position shown
in Figure 18, and the billet curved from right to left as predicted.
The initial explanation proposed seemed to be correct that if the slip
directions available were not symmetrical with respect to the rolling
direction, as in the [111](1T0), then the most favorable slip directions
for forward material propagation would be to one side of the billet. This
material transport to one side of the billet would cause greater material
generation on one side than on the other. The constraint of the material
deficient side to which it is joined would then cause the billet to roll
in a curved shape. For the orientation of the unit cube shown in Figure
18, the material deficient side of the [111](1T0) billet should be the
left side causing the billet to curve from right to left. Knowing this
then a billet could be reduced without exaggerating the curving with each
successive pass by reversing the billet end for end after each pass but
keeping the top surface up. This would allow the material deficient side
to gain material. Several reductions were made on the [111](1T0) billet
using the above compensating technique and the crystal did straighten out.
A complete reduction to 92% was not attempted.

C. Final Rolling Results

Only 1616-14 [011](100) crystal billet from the first five rolled
made the full reduction to 92%. Crystal 1616-30 [100](001), although
rolling successfully, was scrapped because its sub-size dimensions would
not yield sufficient material for a satisfactory sheet evaluation, and
insufficient time remained to roll a billet of the [111](1T0) rolling
geometry and compensate for the curving defect described above.

Three other crystal billets from the group were introduced into
the rolling program as substitutes for the fractured crystals. These
three plus 1616-14 [011](100) constituted the material rolled successfully
to a 92% reduction in thickness with only minor difficulties, finally ob-
taining the following dimensions.

Billet No.	Rolling- Direction & Plane	Thick(in.)	Width(in.)	% Red. in Thickness
1616-14	[011](100)	0.018	0.670	92%
1616-50	[011](0T1)	0.021	0.70	91%
1616-65	[100](001)	0.019	0.650	92%
1616-70	[100](011)	0.017	0.530	93%

Lengths of the above billets are not noted since samples cropped at various reductions made a final rolled length meaningless. A view of the final mill product obtained from the four billets is shown in Figure 19. It was noted that some edge cracking occurred on 1616-65 [100](001) and on 1616-14 [011](100). The breaking of 1616-70 [100] (011) was the result of handling the material and did not occur during rolling. The edge cracking in the two former specimens was caused by a low rolling temperature at the reduction obtained. Edge cracking was noted in 1616-14 [011](100) after an 87% reduction at which point the rolling temperature was decreased from 650°C to 400°C. This final temperature in the schedule had to be raised from 400°C to 500°C finally to 600°C before the billet would take reductions from 87% to 92% without edge cracking. Using this experimentally amended rolling temperature schedule stated earlier, rolling took place with a minimum of difficulty.

IV. EVALUATION OF SHEET MATERIAL ROLLED FROM TUNGSTEN SINGLE CRYSTALS

A. Recrystallization Temperature

The determination of recrystallization temperatures for various reductions on the four oriented billets rolled successfully to the 92% stage was central in this study. The definition of recrystallization used was the formation of stress-free, equiaxed grains in a matrix showing no signs of grain growth. Recrystallization temperature was defined to be that temperature to which samples were heated for one-half hour that produced a recrystallized matrix. The attainment of a stress-free, equiaxed grain structure showing no signs of grain growth was determined using visual microscopic examination and Knoop microhardness measurements.

Samples for this study were cut from the as-rolled sheet using a water-cooled cut-off wheel, heated to the desired temperature in a vacuum furnace for 1/2 hour, and cooled in vacuum to room temperature, mounted to allow viewing of the transverse (normal to the rolling direction) and longitudinal (parallel to the rolling direction) cross-sections of the sheet, polished using standard metallographic procedures, and etched using Murakami's Reagent.

Photomicrographs of the four billets at an 87% reduction are shown in the as-rolled condition, below recrystallization temperature, at recrystallization, and showing grain growth in Figures 20, 21, 22, and 23 as being typical of the microstructures viewed of the sheet samples.
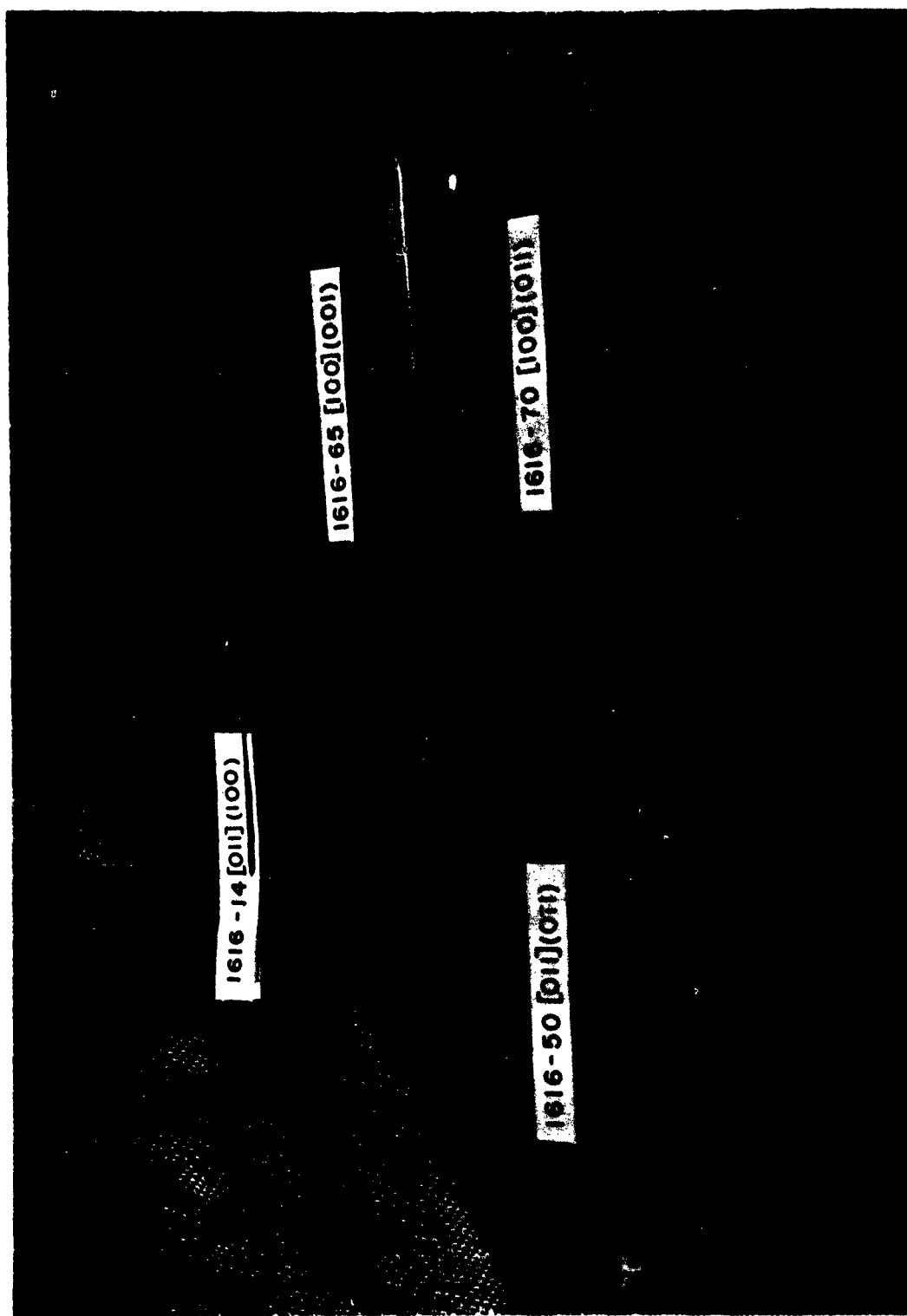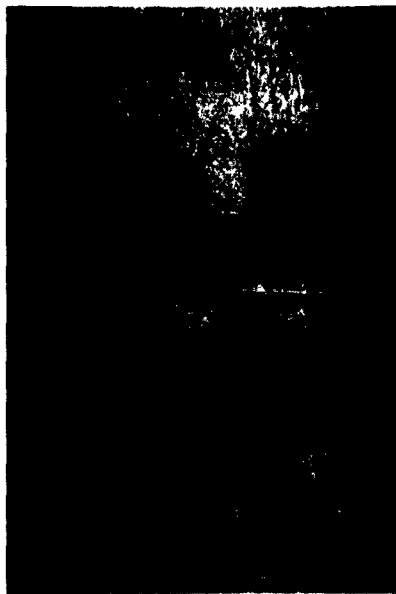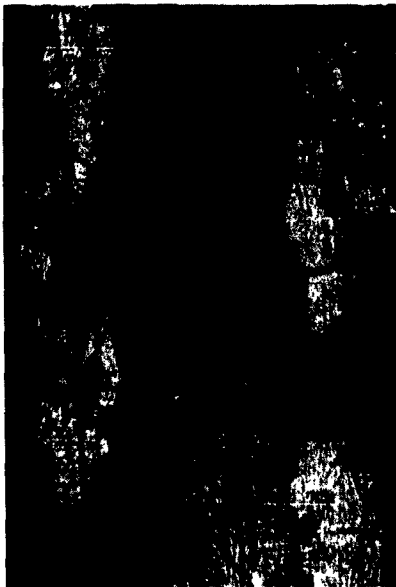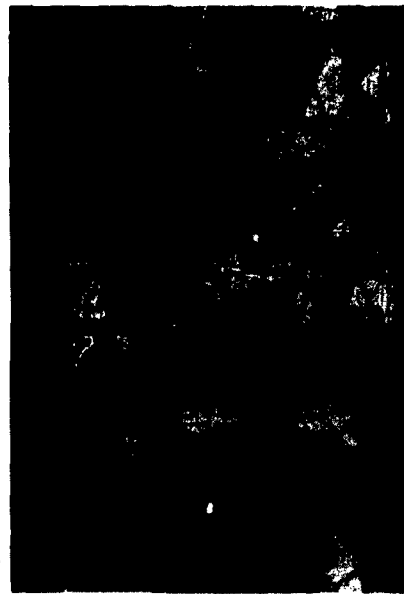
- 29 -

Figure 19. Final Mill Product of Four Tungsten Billets Reduced 92% in Thickness.

b. Pre-recrystallization 1400°C, Longitudinal View.

d. Grain Growth 1700°C, Longitudinal View.

a. As-rolled, Transverse View.

c. Recrystallized Matrix 1550°C, Longitudinal View.

Figure 20. Photomicrographs of Four Phases of the Recrystallization Process for Billet 1616-14 [011](100) 87% Reduction, Mag. 100x Etchant; Murakami's.

a. As-rolled, Transverse View.
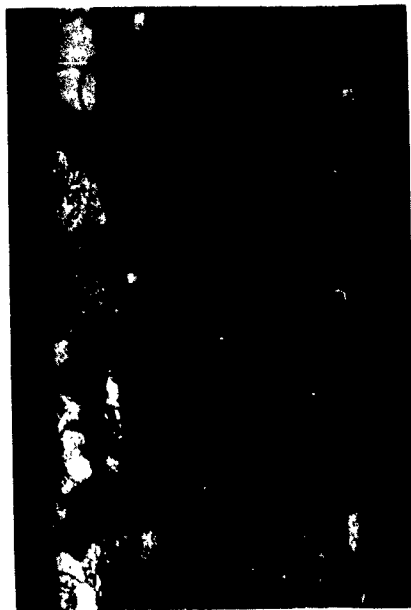
b. Pre-recrystallization 1300°C, Longitudinal View.

c. Recrystallized Matrix 1500°C, Transverse View.

d. Grain Growth 1700°C, Longitudinal View.

Figure 21.   Photomicrographs of Four Phases of the Recrystallization Process for Billet 1616-65 [100](001) 87% Reduction, Mag. 100x Etchant; Murakami's.

b. Pre-recrystallization 1200°C, Transverse View.

d. Grain Growth 1600°C, Longitudinal View.

a. As-rolled, Transverse View.

c. Recrystallized Matrix 1500°C, Longitudinal View.

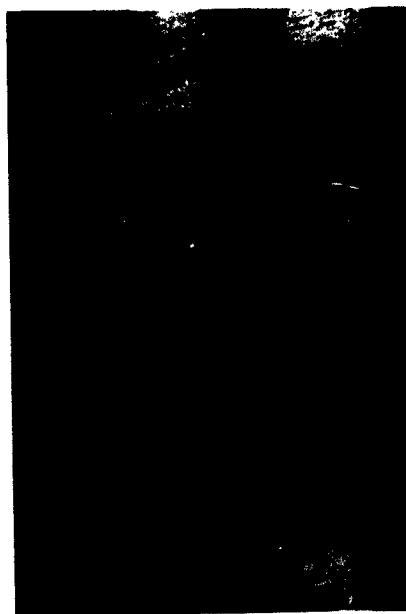Figure 22. Photomicrographs of Four Phases of the Recrystallization Process for Billet 1616-70 [100](011) 87% Reduction, Mag. 100x Etchant; Murakami's.

b. Pre-recrystallization 1200°C, Transverse View.

d. Grain Growth 1600°C, Longitudinal View.

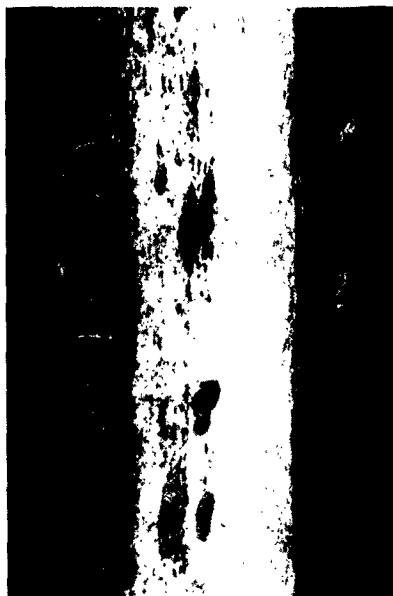a. As-rolled, Transverse View.

c. Recrystallized Matrix 1300°C, Longitudinal View.

Figure 23. Photomicrographs of Four Phases of the Recrystallization Process for Billet 1616-50 [011](0$\bar{1}$1) 87% Reduction, Mag. 100x Etchant; Murakami's.

Graphics displaying the average Knoop hardness values vs. temperature are shown in Figures 24, 25, 26, and 27 for each of the four billet orientations with percent reduction in thickness as a parameter. The hardness tests were taken on transverse cross-sections of the sheet with the longest dimension of the Knoop Indentor parallel to the width dimension in the sheet. This meant general levels of hardness would be different for the various billets of different orientation, since strength, and therefore hardness, are anisotropic properties. The anisotropy shown in this measurement caused significantly varying hardness values in going from grain to grain in the partially, fully, and secondarily-recrystallized matrices. These variations were widest in material given lesser reductions, 50 to 70% in thickness, and in the orientations thought to be unstable in texture either during rolling and/or in the cold-worked to recrystallized structure transition.

The recrystallization temperature was determined from these curves to be the temperature producing the minimum hardness value and correlating this with the visual observation of the microstructure.

No effort was made to determine the recrystallization temperature value to closer than $\pm 50^{\circ}C$ due to the difficulty in trying to distinguish between microstructures given annealing treatments differing only by 50° and inability to closely control the vacuum furnace temperature. A compilation of the recrystallization temperatures determined by hardness and visual measurements is shown in Figure 28 for the four rolling orientations at the various reductions at which samples were taken.

The results shown follow the behavior expected at the outset of the study and can be explained using the models of the unit cube orientation in the various billets, the slip systems proposed, and the relative levels of the stress values acting on these slip systems as reported in the stress calculations.

The [011](100) geometry of 1616-14 had the highest recrystallization temperature at all stages of reduction which indicates the coplanar slip directions-rolling force-rolling direction (shown in Figure 5), the number of operative slip systems, and the high resolved values of the compressive rolling stress necessary to cause slip allowed an easier deformation with apparently less stored energy in the matrix through this "easy rolling mode" making possible a higher recrystallization temperature.

The [100](001) geometry of 1616-65 ranked second in the recrystallization temperature at the four sampled stages of reduction. The number of operative slip systems and values of stress necessary to operate these systems was identical to the [011](100) geometry of 1616-14. The one difference as seen in the model was the rolling force-rolling direction-slip direction vectors were not coplanar. The results would indicate the lack of this "easy rolling mode" made a difference.

FIGURE 24

ROOM TEMPERATURE HARDNESS VS HALF HOUR ANNEAL TEMPERATURE
FOR 1616-14 [011] (100) WITH PERCENT REDUCTION AS A PARAMETER.

FIGURE 25

ROOM TEMPERATURE HARDNESS VS HALF HOUR ANNEAL TEMPERATURE FOR 1616-65 [100] (001) WITH PERCENT REDUCTION AS A PARAMETER.
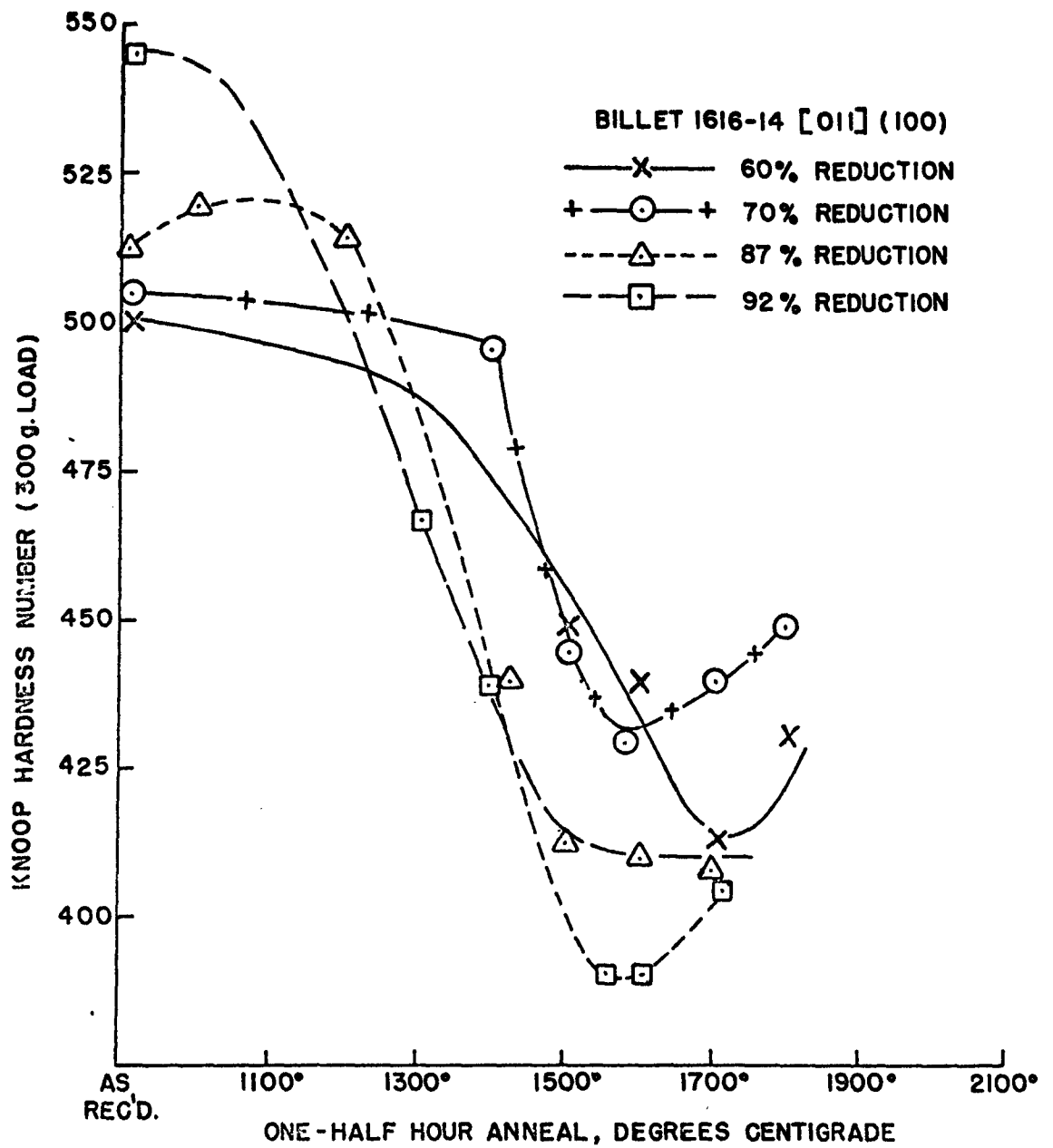
- 37 -

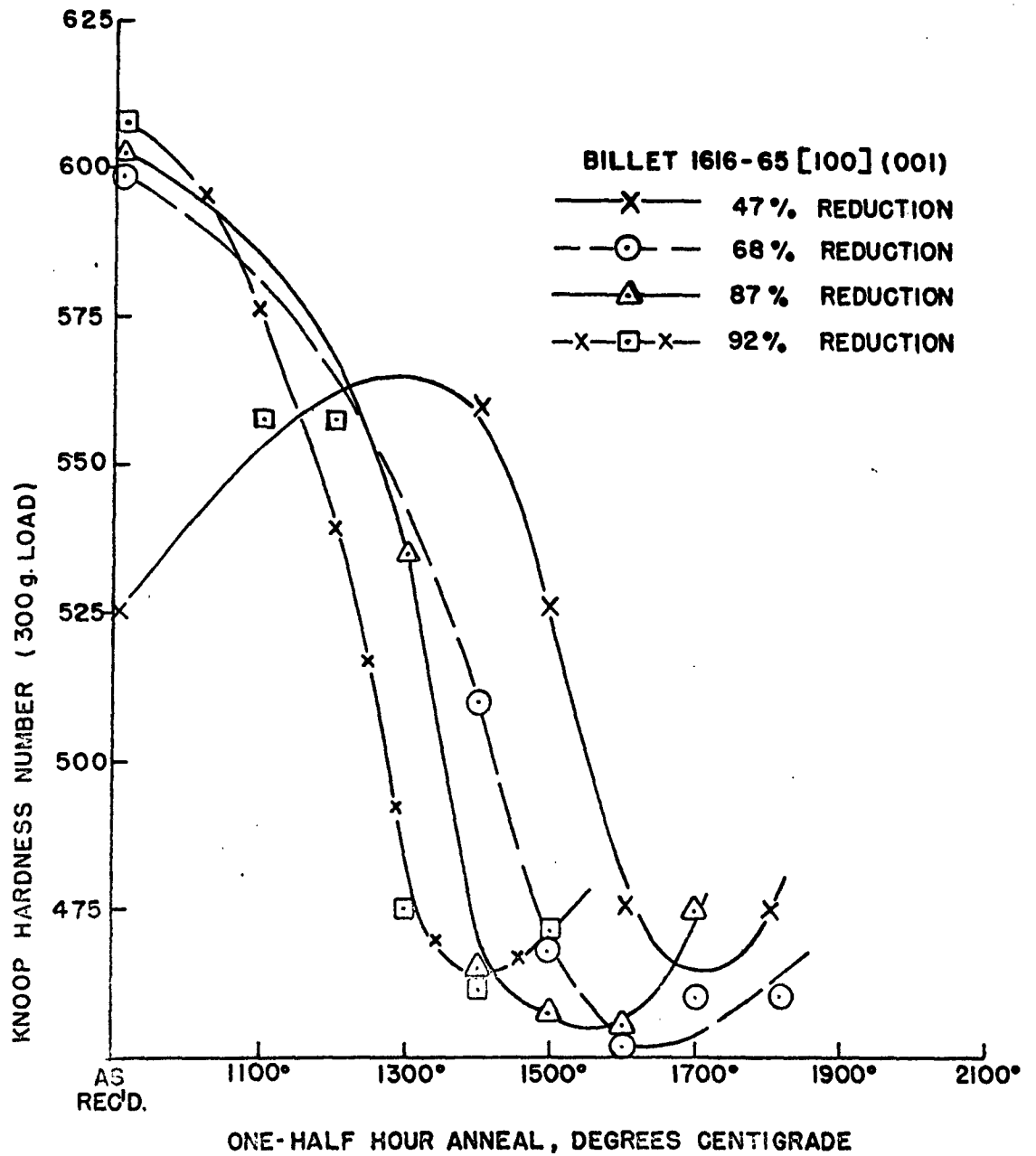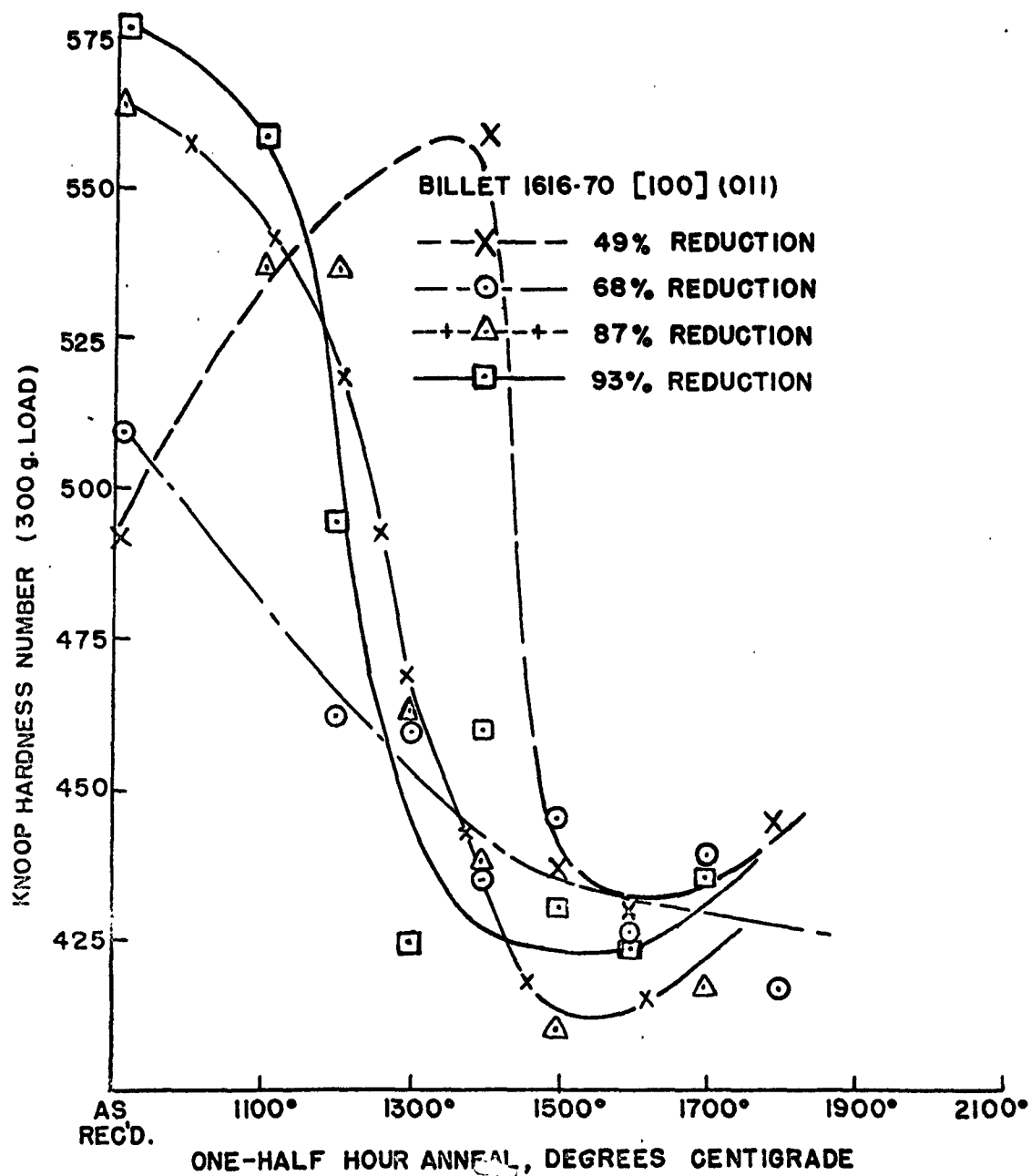FIGURE 26

ROOM TEMPERATURE HARDNESS VS HALF HOUR ANNEAL TEMPERATURE
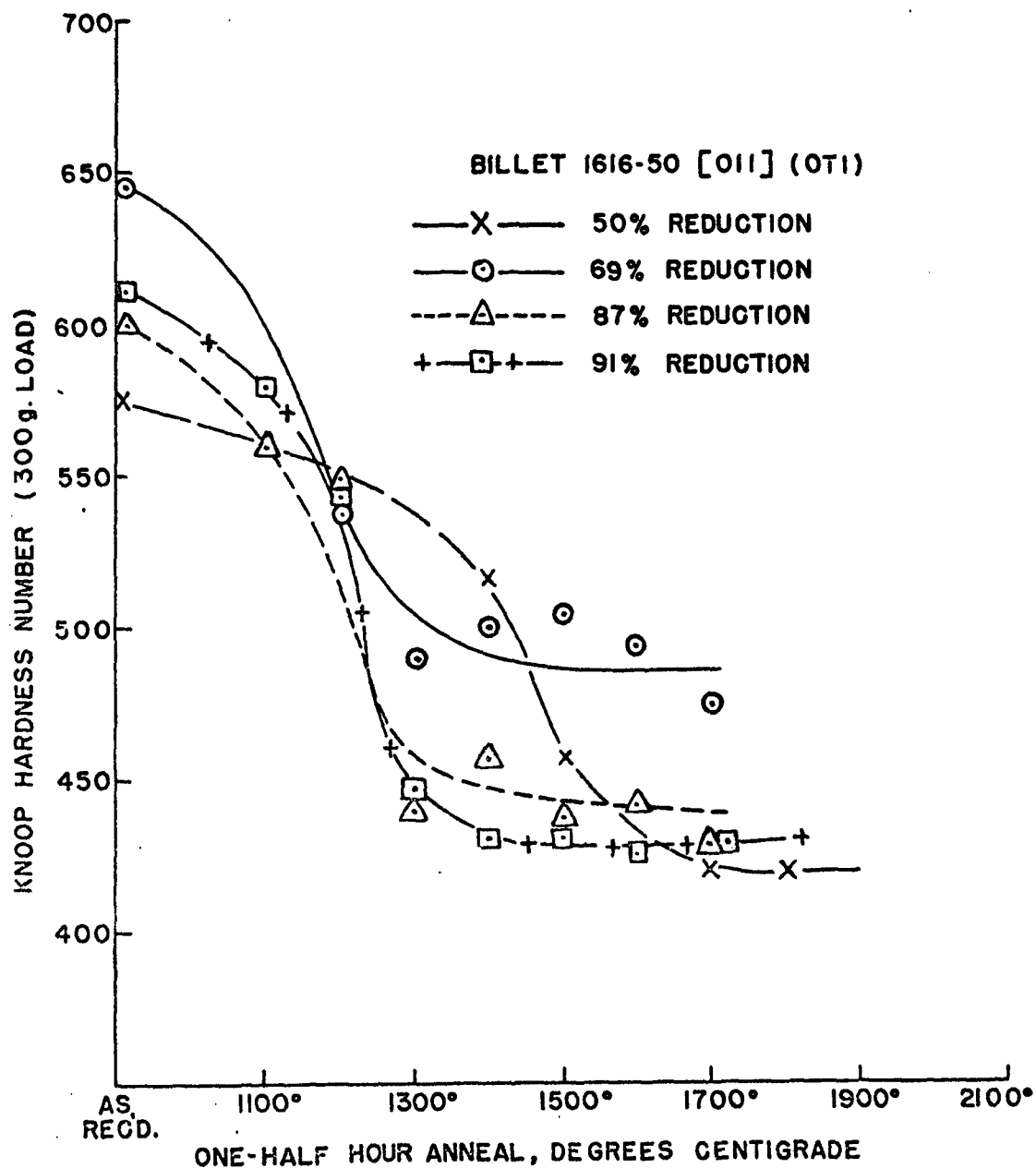FOR 1616-70 [100] (011) WITH PERCENT REDUCTION AS A PARAMETER.

FIGURE 27

ROOM TEMPERATURE HARDNESS VS HALF HOUR ANNEAL TEMPERATURE FOR 1616-50 [011](OTI) WITH PERCENT REDUCTION AS A PARAMETER.
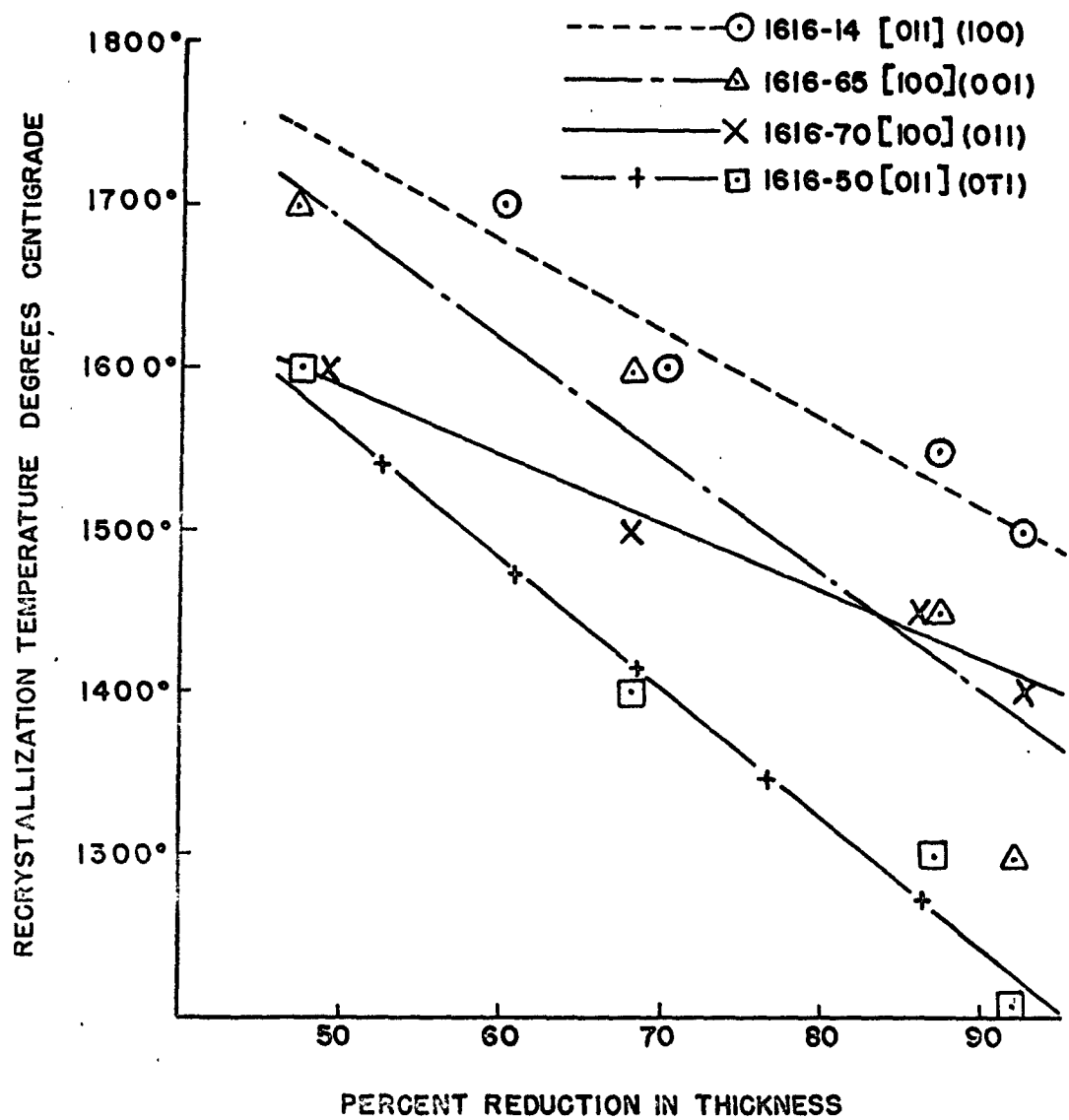
FIGURE 28

RECRYSTALLIZATION TEMPERATURE VS PERCENT REDUCTION
IN THICKNESS WITH BILLET ROLLING DIRECTION - ROLLING
PLANE AS A PARAMETER.

The [100](011) geometry of 1616-70 is third in order of recrys-
tallization temperature at the reductions sampled except at the highest
reductions where it seems to rival the [100](001) geometry of 1616-65
for ease of deformation and therefore degree of matrix stored energy.
The number of slip planes capable of activation are inferior in the
[100](011) geometry compared to the [100](001). However, the reason
it may be equal to the [100](001) at reductions of 87% and 92% is that
[100](011) has for a portion of its slip system the coplanar rolling
force-rolling direction and a pair of slip directions; namely, the [100]
rolling direction, the [011] force direction, and the [111] and [Ī11] slip
directions, an "easy rolling mode". This allows a reasoning similar to
that used in [011](100) geometry over the [100](001) above.

The [011](0Ī1) geometry of 1616-50 had the lowest recrystallization
temperature at each of the reductions sampled of any of the billet rolling
orientations. It was lower than 1616-70 [100](011) even though both con-
tained the same number of active slip systems and the same values for re-
solved shear stress. The 1616-50 [011](0Ī1) billet had no easy deformation
directions coplanar with a force and rolling directions.

B. Recrystallization Mode & Grain Size Determination

An interesting observation made on the four rolling geometries
was that recrystallization was initiated in two different ways.

Billet	Rolling Dir. -Rolling Plane	Mode of Initial Recrystallization
1616-14	[011](100)	Surface Initiated
1616-65	[100](001)	Surface Initiated
1616-70	[100](011)	Initiated in Interior along Deformation Bands
1616-50	[011](0Ī1)	Initiated in Interior along Deformation Bands

Listed above in order of decreasing recrystallization temperature, the two
billets having the highest recrystallization temperature have only surface
initiated recrystallization as shown in Figures 20b and 21b of these two
orientations heated to temperatures below those necessary to cause complete
recrystallization. This might indicate that during deformation these orien-
tations contained sufficient easy slip systems that distortion was greatest
at the surface due to constraint of this material by the rolls. The other
two billets with lower measured recrystallization temperatures also showed
initial signs of recrystallization near the surface, but primarily the
first crystallites were seen along deformation bands in the interior as
seen in Figures 22b and 23b. This would indicate that greatest distortion
occurred in the few regions where slip could occur in these less favorably
oriented billets, which would be shown as heavy slip bands.

A second observation made during the recrystallization studies was that the recrystallized sheet specimens showed varying as well as mixed-grain sizes among the four billets at the various reductions. Observed and measured using a Whippler eyepiece and matching the square grid size with grain size, the following diameters were estimated on samples heated to their recrystallization temperatures.

TABLE V

GRAIN SIZE DETERMINATION IN THE FOUR BILLETS

AT FOUR SAMPLED REDUCTIONS IN THICKNESS

Billet	Orientation	Reduction In Thickness	Grain Size Diameter
1616-14	[011](100)	60%	100 - 200 Microns
		70	90 - 200
		87	30 - 150
		92	30 - 100
1616-65	[100](001)	47%	150 - 250 Microns
		68	50 - 70 & 100 - 200
		87	70 - 150
		92	25 - 40 & 70 - 100
1616-70	[100](011)	49%	300 - 400 Microns
		68	150 - 300
		87	60 - 150
		93	60 - 100
1616-50	[011]($0\bar{1}1$)	50%	50 - 70 & 150 - 400 Microns
		69	25 - 40
		87	25 - 40 & 40 - 80
		91	25 - 30 & 40 - 70

In Table V, the results show a decrease in recrystallized grain size with increased reduction in thickness. This would follow since more nuclei for initiating recrystallization should be present following increased amounts of deformation. Further, the large grain size in 1616-70 when compared to the grain sizes of 1616-14 and 1616-65 could be explained by the idea of easy slip occurring in the latter two giving rise to numerous sites for nucleation to occur. The billets with less favorable and less numerous slip systems such as 1616-50 and 1616-70 should then contain fewer sites for nucleation to occur and consequently produce a large grain size. However, 1616-50 was fine-grained possibly indicating that cross-slip or a similar mode was occurring in this unfavorable rolling orientation making many more sites for nucleation favorable.

C. Physical Property Testing

Initially it was hoped that tensile specimens, as shown in Figure 29, could be machined from sheet samples cropped off the rolling billet at various reductions in thickness which would show the changes in ductility, tensile and yield strengths with increased cold-work, as well as show clearly the difference in strength levels among the various orientations caused by the anisotropy of the crystal. However, the method used initially ruined several sheet sample lengths of the thicker tungsten sheet. The tensile specimens were produced in multiple specimen packs of tungsten sheet separated with steel strips by grinding the gauge width and radii on one side, then grinding similarly on the reverse side. However, when the second grinding was attempted, the samples would break at some point in the gauge length. In an attempt to eliminate this, DeKhotinsky cement was utilized not only as a support material in this undercut region during the second grinding to eliminate the beam loading effect, but also between the steel and tungsten plates to form a strong laminate. The resulting packs were successfully ground and the support from the cement-to-steel bond prevented the beam loading on the tungsten strip from reaching the values necessary to cause fracture. Six samples were successfully produced this way.

The tensile tests were run on a Tinius-Olsen electromatic unit at room temperature. A constant strain-rate of 0.002 in./in./min. was used in an effort to eliminate the strain-rate variable so as to more clearly point up orientation differences. The tests showed differences existed in values of strength or ductility among the orientations sampled. Of the six specimens tested, five were of non-uniform thickness making gripping difficult, one of these broke in the first stages of the test unexplainably, and one specimen was found to be slightly delaminated on one edge during the grinding to size and broke at almost a no-load condition. The curves are shown for the four specimens tested in Figure 30.

The results shown in Figure 30 and Table VI are as expected except for the low ductility value in the [011](100) 1616-14 billet. This should not occur in this supposed easy deformation rolling orientation in conjunction with the low yield strength and ultimate tensile strength. The remaining samples exhibit the relative strength levels expected; however, the strain values and resulting ductility and modulus values calculated all are lower than expected. A partial explanation for this anomalous behavior might lie in the sub-surface cracks lying along deformation bands which would cause local catastrophic failure greatly affecting the strain values and contributing to low strengths and low ductility values.

A second and more conclusive indication of the dependence of physical properties on orientation is a graph of as-rolled hardness vs. percent reduction in thickness taken on a transverse cross-section with the indentor length parallel to the width dimension of the sheet shown

SCALE = 10 X
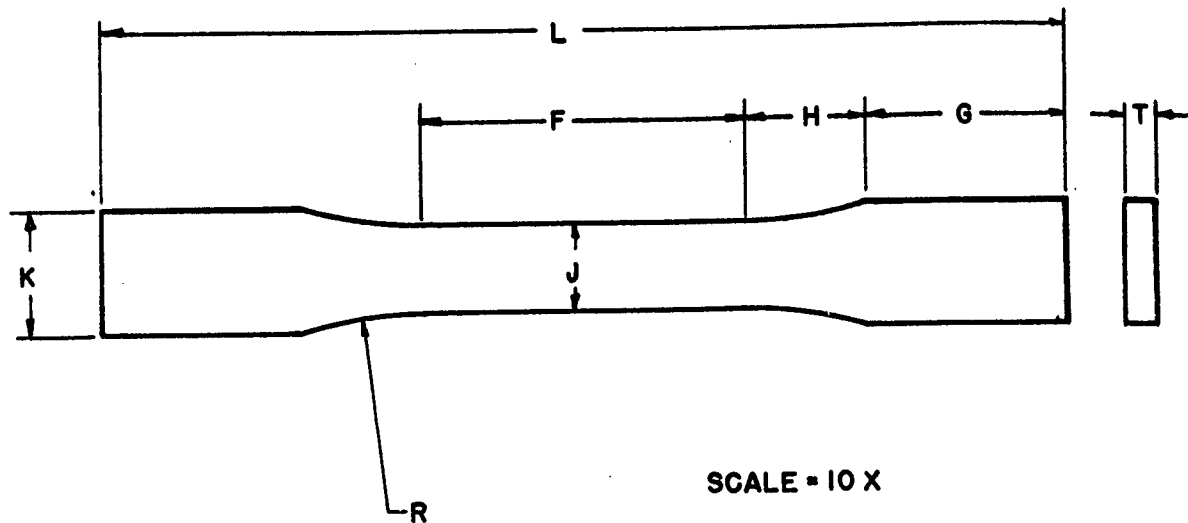
SYMBOL	DESIGNATION	DIMENSION
F	GAGE LENGTH	2.000" ± 0.010" TANG. TO TANG.
G	GRIP LENGTH	0.391" ± 0.010" TANG. TO EDGE
H	TANGENT DISTANCE	0.609" ± 0.001" TANG. TO TANG.
J	GAGE WIDTH	0.250" ± 0.001" POLISHED LONGITUD.
K	GRIP WIDTH	0.375" ± 0 010"
L	SPECIMEN LENGTH	4.000" ± 0.010"
R	RADIUS FILLET	3.000" ± 0.001" POLISHED LONGITUD.
T	THICKNESS	THICKNESS OF MATERIAL

FIGURE 29
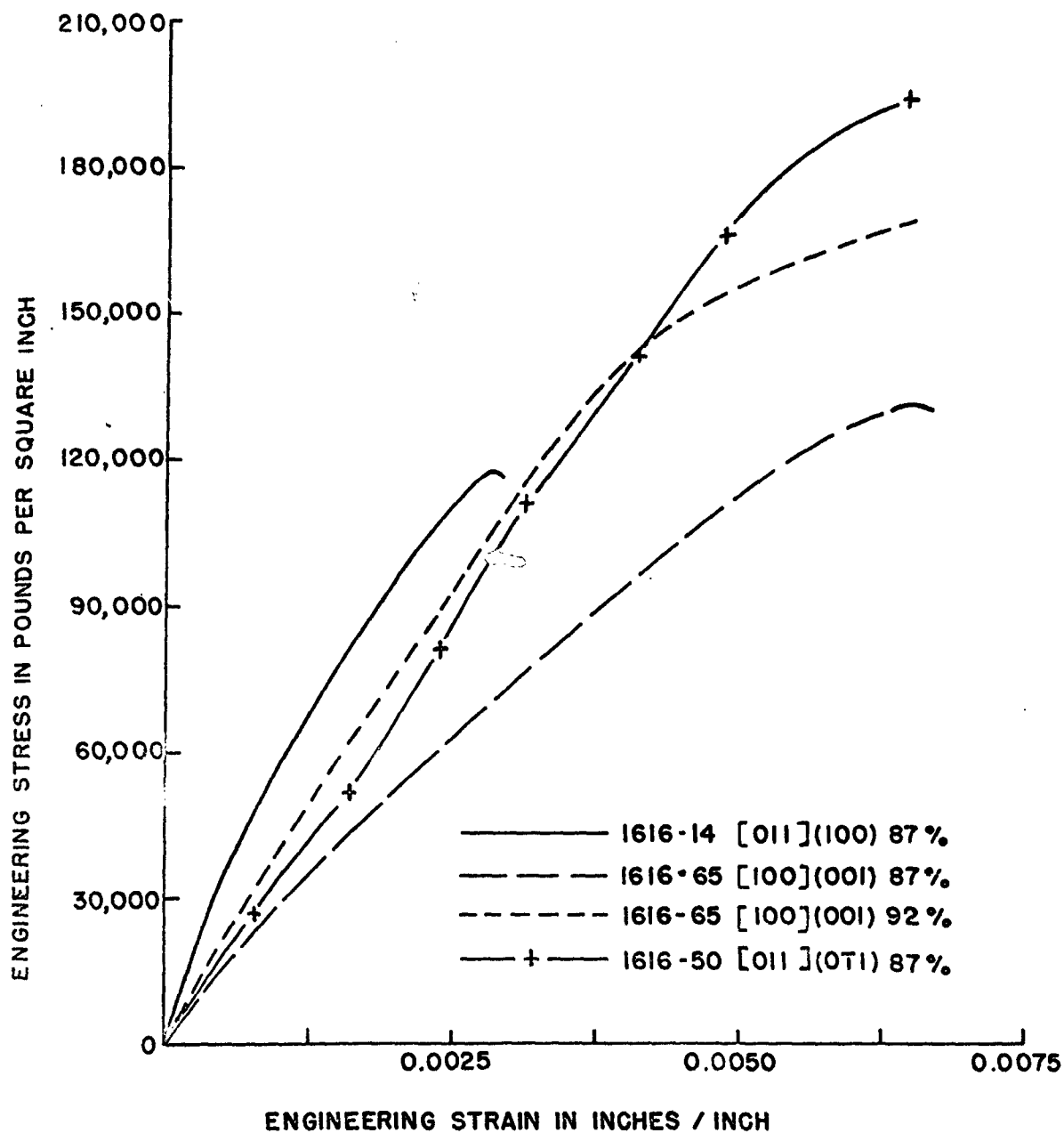
SPECIMEN DIMENSIONS OF SHEET TENSILE SPECIMEN

FIGURE 30

TENSILE TEST CURVES FOR AS-ROLLED TUNGSTEN SHEET SPECIMENS USING 0.002 INCHES / INCH STRAIN RATE.

TABLE VI

ROOM TEMPERATURE TENSILE TEST DATA

Billet	Orientation	% Red.	0.05% Off-set Yield Strength	Ultimate Tensile Strength	% Elong.	Young's Modulus
1616-14	[011](100)	87%	97,500 psi	120,000 psi	0.275%	60×10^6 psi
1616-65	[100](001)	87	145,000	145,000	0.65	24×10^6
1616-65	[100](001)	92	147,000	168,000	0.625	35×10^6
1616-50	[011](0$\bar{1}$1)	87	174,000	192,000	0.625	36×10^6

in Figure 31 with rolling orientation as a parameter. This further
bears out the strength figures obtained on the sheet tensile specimens
at an 87% reduction in thickness. In addition, it shows a tendency for
the [100](011) and [011](0$\bar{1}$1) geometries to work-harden at nearly the
same rate. However, they work-harden at a faster rate than the [011](100)
and [100](001) geometries which, incidentally, work-harden at similar rates
as shown by the slopes of the two curves for 1616-14 and 1616-65. This
behavior again follows from the slip planes operable in each of the four
orientations of the unit cube in the billet rolling plane-rolling direc-
tions investigated.

CONCLUSIONS:

Initial billet orientation influences the recrystallization tempera-
ture of sheet rolled from tungsten single crystals. Of the four orienta-
tions investigated by warm-rolling to a 92% reduction in thickness with
no annealing treatments between passes, the [011](100) orientation of
billet 1616-14 had the highest recrystallization temperature at all reduc-
tions sampled. The [100](001) orientation of 1616-65, the [100](011)
orientation of 1616-70, and the [011](0$\bar{1}$1) orientation of 1616-50 followed
in decreasing order.

These results compare favorably to those obtained on the body-center
cubic system of iron-3% silicon.[1] This behavior seems to be related to
1) the number of slip systems acted on by high values of resolved compres-
sive stress calculated using Equation 1 above, and 2) the existence of an
"easy rolling mode" in which the direction of slip in a slip system and the
rolling direction are coplanar with the direction of applied force. Condi-
tion (2) causes one rolling orientation to be superior to another in recrys-
tallization temperature if both are equal under condition (1). For two
rolling orientations differing in condition (1), the orientation having the
greater number will have the higher recrystallization temperature. For two
rolling orientations, one with a higher number of slip systems operable and
the other with fewer slip systems operable but "easy rolling modes" opera-
ting on those available, the recrystallization temperatures would be nearly
the same.

Billet orientation affects the mode of initial recrystallization and
the as-recrystallized grain size. The reasons for this are felt to be
tied to a more complex deformation mode than is shown in the model above;
however, they are felt to be related to the deformation of the oriented
single crystal, the number of slip planes operable, interactions between
slip systems, and the presence or absence of "easy rolling modes".

Finally, billet orientation affects the rate of work-hardening of
the tungsten sheet during rolling when the same decrements and rolling
temperatures are used. This, in turn, affects the physical properties
of the sheet; hardness, tensile strength, and ductility, with hardness
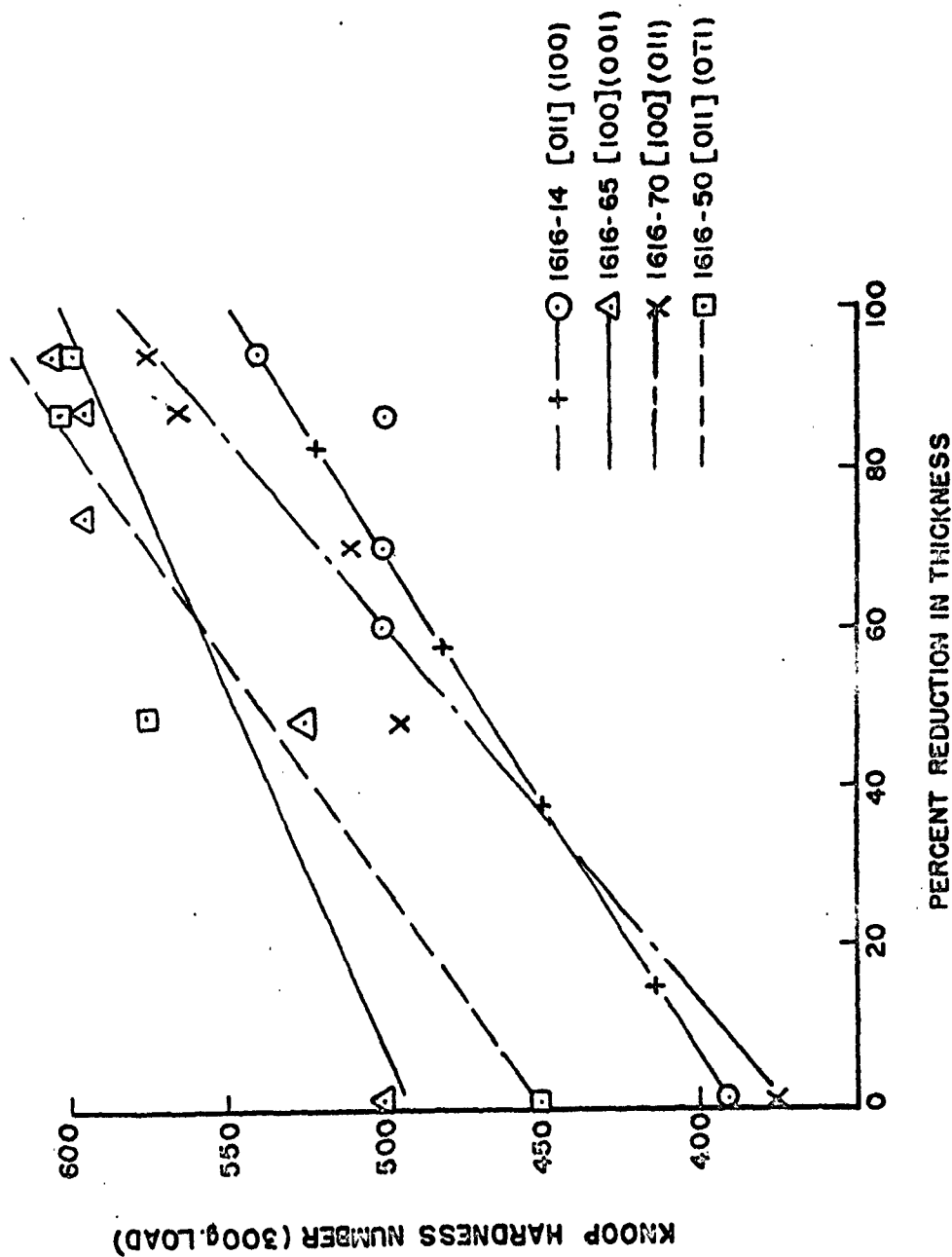being the property most accurately measured.

FIGURE 31

AS ROLLED HARDNESS VS PERCENT REDUCTION IN THICKNESS TAKEN ON TRANSVERSE
CROSS SECTION WITH INDENTOR LENGTH PARALLEL TO PLANE OF ROLLING WITH
ROLLING DIRECTION –ROLLING PLANE AS A PARAMETER.

RECOMMENDATIONS FOR FUTURE WORK:

A. Sheet Texture Study

From the study above it may be seen that initial billet orientation does influence the recrystallization temperature, recrystallization mode, recrystallized grain size, and strength values. However, questions remain about the final orientation of the sheet or texture. It is known from the silicon-iron study that b.c.c. single crystal orientations deformed by rolling are not all stable. Some initial orientations are changed during rolling to a new rolling plane-rolling direction. Some orientations undergo a change to a different texture upon recrystallization, while some remain unchanged throughout rolling and recrystallization. While it is felt the orientations which would do this are predictable based on favorable slip systems in the various rolling plane-rolling direction combinations, an X-ray study of the sheet textures produced during rolling and annealing would be necessary to show conclusive results.
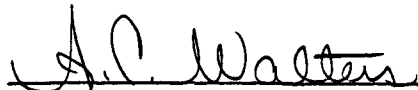
B. Billet Scale-up

The sheet product produced from the 1/4-inch by 3/8-inch by 6-inches single crystal tungsten billets rolled to a ribbon only a little over 1/2-inch wide. For a sheet product of better utility, single crystal billets several inches wide must be produced. An exploratory effort in this line led to the rectangular-shaped crystal in rough billet form shown in Figure 7. This crystal, although not a perfect single crystal in the cross-section, shows feasibility exists for producing this material in a larger single crystal form. This scale-up should be further exploited to produce billets 4-inches wide by 3/8-inch thick by 20-inches long for the production of wider sheet of controlled orientation and texture.

C. Alloy Program

To further increase the recrystallization temperature of the tungsten sheet rolled from single crystals, an investigation of the rolling of doped single crystals and the resulting properties would seem desirable. Doping elements such as rhenium and aluminum effect considerable influence on the recrystallization temperature of wrought tungsten and would make an excellent starting point for an investigation of alloying in tungsten single crystals.

A.C. Walters:nm

- 49 -

REFERENCES

(1)   W.R. Hibbard, Jr. and W.R. Tully, "The Effect of Orientation
       on the Recrystallization Kinetics of Cold-Rolled Single Crys-
       tals," Transactions of the Metallurgical Society of A.I.M.E.,
       Vol. 221, April 1961, pp. 336-343.

(2)   F.A. Goucher, "Studies on the Deformation of Tungsten Single
       Crystals Under Tensile Stress," Philosophical Magazine, 48
       (287), November 1924, pp. 800-19.

(3)   E.M. da C. Andrade, "Slip in Single Crystals - Glide and
       Hardening in Metal Single Crystals," Proceedings of the
       Physical Society, (289), Vol. 52, January 1, 1940, pp. 1-7.

(4)   H.W. Schadler and J.R. Low, Jr., "Annual Summary Report Low
       Temperature Brittleness of Refractory Metals," Contract No.
       Nonr-2614(00), August 1959.

(5)   L.R. Underwood, "The Rolling of Metals," John Wiley and Sons,
       Inc., Vol. I, 1950, p. 11.

(6)   C.E. Harvey, A Method of Semi-Quantitative Spectrochemical
       Analysis, Applied Research Laboratories, Glendale, California,
       1947.

(7)   C.T. Wei, "Zone Reflection Camera for Studying Crystal Imper-
       fections by the Schulz Technique," The Review of Scientific
       Instruments, (6), Vol. 27, June 1956, pp. 397-99.

RESEARCH LABORATORY

FINAL TECHNICAL REPORT

RECRYSTALLIZATION OF WORKED SINGLE
CRYSTALS OF TUNGSTEN

Prepared for: Linde Company
                                 A Division of Union Carbide Corporation
                                 Indianapolis, Indiana

Under Subcontract
No. 1 to Prime Contract: NOw 61-0671-c
                                 Purchase Order No. LAB 34867

Prepared by: W. G. Reuter
                                 L. Raymond
                                 E. L. Harmon

21 August 1963

AERONUTRONIC DIVISION   Newport Beach,
PHILCO CORPORATION   California

CONTENTS

PART I

ILLUSTRATIONS

ILLUSTRATIONS (Continued)

ILLUSTRATIONS (Continued)

PART I

SECTION I-1

INTRODUCTION

The objectives of this investigation are two-fold. The
first part of this report will be concerned with the requests of the
Linde Company to employ the Aeronutronic hot-rolling facilities to
deform tungsten single crystals.

The tungsten crystals of different orientations were deformed
different amounts at different temperatures by rolling as prescribed by
the Linde Company. The details of each operation are presented for each
crystal which is identified by code number and the corresponding rolling
plane and rolling direction. Comments, applicable to each specific
conditions, are included.

SECTION I-2

EXPERIMENTAL PROCEDURE

I-2.1 ROLLING FACILITIES

The rolling mill (Figure 1) is a Loma Model 600 which has been modified to permit operation at elevated temperatures. Throughout the program, the temperature of the rolls was between 700 and 850°F.

Prior to rolling, all specimens were heated to a predetermined temperature. As shown in Figure 2, a tubular furnace with an argon atmosphere was used to maintain the temperature which was recorded by a Pt-PtRh thermocouple and an L&N potentiometer.

I-2.2 ROLLING OPERATION

Scrap tungsten crystals one-half inch round by six and one-half inches long were used to determine if there are any inherent limitations in the equipment when rolling tungsten single crystals. The results of different rolling sequences are shown in Table I.

As readily observed from the results of Table I, deformations to about 90 per cent can be obtained without any fracture occurring on rolling. Deformations of 20 per cent per pass on the as-received crystals are readily attainable with the temperatures maintained throughout the operation quite adequate for facile processing. A limitation in the rolling operation, which was detected later in the program, was a 0.020 inch minimum crystal thickness after rolling. Further reduction could only be accomplished by sandwiching or using a smaller diameter roll on the rolling mill.

TABLE I

DIFFERENT ROLLING SEQUENCES FOR TUNGSTEN SINGLE CRYSTALS

Crystal	Crystal Temperature on Rolling	Original Thickness (inches)	Deformation per pass	Number of Passes	Final Thickness (inches)	Total Percent Deformation
1616-22	1800°F	0.500	.050	7	0.150	70
	1800°F	0.150	.010	4	0.110	78
	1800°F	0.110	.008	5	0.070	84
1616-24	1750°F	0.500	.100	3	0.200	60
	1750°F	0.200	.050	1	0.150	70
	1750°F	0.150	.010	4	0.110	78
	1640°F	0.110	.008	5	0.070	84
1616-36	1800°F	0.500	.100	1	0.400	20
	1800°F	0.400	.075	2	0.250	50
	1800°F	0.250	.050	2	0.150	70
1616-36A	1820°F	0.150	.010	3	0.118	76.0
	1660°F	0.118	.008	6	0.070	84.0
	1480°F	0.070	.004	7	0.042	91.6
	1260°F	0.042	.102		0.041 (fractured)	
1616-36B	1820°F	0.150	.027	1	0.123	75.4
	1660°F	0.123	.046	1	0.077	84.6
	1480°F	0.077	.023	1	0.054	89.2
	1260°F	0.054	.010	1	0.044 (fractured)	

An aligning fixture was used to position the crystals in the center of the rolls. A clean set of rolls gave optimum results. The width of the crystal had very little tapering from the center to the edge. The length of the crystal had a maximum deviation of ±.001 for the longer samples. With use, a groove gradually appeared in the center of the rolls. As the groove progressively got worse, the width of the crystals began to taper from center to edge. Several times a crystal would leave an imprint on the rolls and subsequent passes would mark the following samples, as readily seen in Figures 6 and 8. It was found that a wide piece of steel rolled through the mill would remove the imprints from the rolls.

To avoid rolling oxides into the sample between passes, the surfaces were adequately cleaned with a boiling solution of 20 per cent KOH. Use of hydrogen gas at 1800°F was found to be inadequate as a cleaning agent.

I-2.3 CRYSTAL DEFORMATION

The tungsten single crystals supplied by the Linde Company were in the form of a rectangular parallelepiped. As requested by Linde, the same crystal orientation relative to the rolls was used on each pass, i.e., the specimen was fed into the rolls with the same lead end with no rotation of the crystal. It was hoped that the rolled crystals would result in straight pieces which later could be machined into tensile specimens. Any curvatures in the specimens due to rolling would therefore be undesirable. The test pieces were returned to the Linde Company, after the prescribed rolling operation was completed.

SECTION I-3

RESULTS

The tungsten single crystals were deformed in the following
sequences:

1616-30A   (001)   [100]

The crystal, whose original length was 3.3 inch, was rolled
at 1740°F (949°C) from 0.132 inch thick to 0.095 inch thick in one
pass. A 1½ inch long sample was cut off the aft end and sent to the
Linde Company. The remaining crystal was rolled to 0.058 inch thick
in five passes at 1610°F (876°C) then to 0.040 inch thick in four
passes at 1476°F (802°C) and to 0.023 inch thick in eight passes at
1205°F.(651°C). The sample began to curl as shown by the long crystal
in Figure 3. The straight portion of the lead end, left side in
Figure 3, was cut off and subjected to one more pass at 1205°F to 0.022
inch thick. No further reduction could be obtained because of the
limitation in the rolling mill.

1616-30B   (001)   [100]

The length of the second crystal was 2.25 inches prior to
rolling. At 1745°F the thickness was reduced from 0.132 inch to
0.095 inch thick in one pass. Five passes were used at 1610°F to
reduce the thickness to 0.058 inch after which a 1½ inch sample was
cut off the aft end and sent to the Linde Company. The remaining
crystal was then rolled to a final thickness of 0.021 inch in 11 passes
at 1205°F. The final piece is shown by the short piece in Figure 3.

1616-65   (001)   [100]

The crystal was originally 6 inches long and 0.253 inch thick.
The first reduction to 0.176 inch was accomplished in three passes at

$1745^{\circ}F$. At $1610^{\circ}F$ four passes reduced the thickness to 0.134 inch. The specimen was still relatively straight and about 9½ inches long (Figure 4). A 1¼ inch long sample was cut off the aft end and sent to the Linde Company. At $1475^{\circ}F$, six passes were used to reduce the thickness to .080 inch. The sample, shown in Figure 5, had a five inch piece cut off the aft end which was sent to Linde and the remaining crystal was still straight. After six passes at $1205^{\circ}F$ the thickness was .048 and the remaining crystal was still straight (Figure 6). Another pass at $1205^{\circ}F$ to .043 caused a severe edge crack, which necessitated cutting the samples in two. The two pieces were rolled to 0.032 inch thick at $1205^{\circ}F$ in three and four passes. The 7 3/4 inch long sample was sent to Linde Company and the rolling continued on the shorter piece. Edge cracking had appeared after the shorter sample was 0.036 inch thick and continued throughout the rolling of the sample. The remaining crystal was rolled from .032 to .019 inch thick in eight passes at $1100^{\circ}F$ $(595^{\circ}C)$.

1616-70 (011) [100]

The six-inch crystal was rolled at $1745^{\circ}F$ from 0.253 inch thick to 0.175 inch thick in three passes. At $1610^{\circ}F$ the crystal was rolled to 0.134 inch thick in four passes.(Figure 7). A 1¼ inch long sample was cut off the aft end and sent to the Linde Company. The remaining crystal was rolled to 0.080 inch thick at $1475^{\circ}F$ in five passes (Figure 8). A 10-inch long sample was cut off the aft end and sent to the Linde Company. The remaining crystal was rolled to 0.036 inch thick at $1205^{\circ}F$ in eight passes. The sample was cut in two at .036 inch thick as a result of a severe edge crack. The two pieces were rolled to .030 inch thick in two passes at $1205^{\circ}F$. The longer of the two pieces, an 8½ inch long piece, was sent to Linde Company. The remaining sample broke in two as a result of a deep mark on the rolls. One of the pieces was rolled from .030 inch thick to .018 inch thick in six passes at $1100^{\circ}F$.

1616-44 (011) [100]

The six-inch crystal was rolled at $1750^{\circ}F$ from 0.238 inch thick to 0.167 inch thick in one pass. The crystal was then rolled at $1610^{\circ}F$ in three passes to .0133 inch thick. At 0.133 inch, the crystal curled in the horizontal and the vertical directions. This piece has been sent to the Linde Company.

-6-

1616-14　(001)　[110]

The six-inch crystal was rolled at 1745°F from 0.234 inch thick to 0.093 inch thick in one pass. A one inch long sample was cut off the aft end and sent to Linde Company. The rest of the crystal was then rolled at 1476°F to 0.083 inch thick in one pass (Figure 9). Another pass was made at 1476°F from .083 inch thick to 0.073 inch thick and a 4½ inch long sample cut off the aft end and sent to Linde Company. The remaining crystal was rolled at 1205°F to 0.032 inch thick in eleven passes and a 9-inch long sample cut off the aft end and sent to Linde Company. The remaining crystal was reduced .001 inch at 755°F (401°C) and a crack appeared at the lead end (Figure 10). A piece one inch long was cut off the front end to remove the crack and the remaining sample reduced .002 inch at 935°F (501°C) and a crack reappeared at the lead end. A one inch long piece was then cut off the lead end to remove the crack and the remaining sample has been rolled at 1100°F in seven passes to a thickness of .018 inch thick. The 1100°F temperature was found adequate to avoid cracks at the lead end.

1616-26　(1̄10)　[110]

The crystal was rolled at 1745°F from an original thickness of 0.158 inch thick to 0.107 inch thick in three passes. A 1½ inch long sample was cut off the aft end and sent to Linde Company. An attempt to reduce the remaining sample at 1610°F to 0.083 inch thick caused the sample to split into two pieces. Figure 11 is a photograph of the final pieces, whose common cleavage plane is the anticipated (001) for tungsten.

1616-50　(01̄1)　[011]

The six-inch crystal was rolled at 1745°F from 0.249 inch thick to 0.181 inch thick in three passes. In five passes the thickness was reduced to 0.131 inch at 1610°F (Figure 12) and a 1½ inch long piece was cut off the aft end and sent to Linde Company. The remaining crystal was rolled to 0.079 inch thick at 1475°F in seven passes (Figure 13) and a 4½ inch long sample was cut off the aft end and sent to Linde Company. The remaining crystal was rolled to 0.033 inch thick at 1205°F in eleven passes. A 4½ inch long sample was cut off for the Linde Company. The remaining crystal was rolled to 0.020 inch thick in eight passes at 1100°F.

If any orientation resisted flow more than the others, it was the (01̄1) [011]. For crystals with identical thickness in the as-received condition, the (01̄1) [011] orientation supplied less reduction for a given roll setting. Although the work hardening coefficient appears to be the highest for the (01̄1) [011], no edge cracking was apparent.

-7-

1616-40 (1$\bar{1}$0) [111]

The six-inch crystal was rolled at 1745°F from an original thickness of 0.238 inch to 0.225 inch. A severe curl resulted in the rolling plane normal to the rolling direction. This crystal has been returned to the Linde Company.

1616-46 (1$\bar{1}$0) [111]

same as above

1616-48 (1$\bar{1}$0) [111]

same as above

1616-42 (1$\bar{1}$0) [111]

After an orientation check by the Linde Company, a fourth sample was subjected to a rolling deformation similar to the previous three. The crystal curled in the direction as predicted by the Linde Company, the sample was then reversed, end-for-end, keeping the same face up and, as expected, the sample straightened out on being subjected to a second pass. The crystal was then returned to the Linde Company.
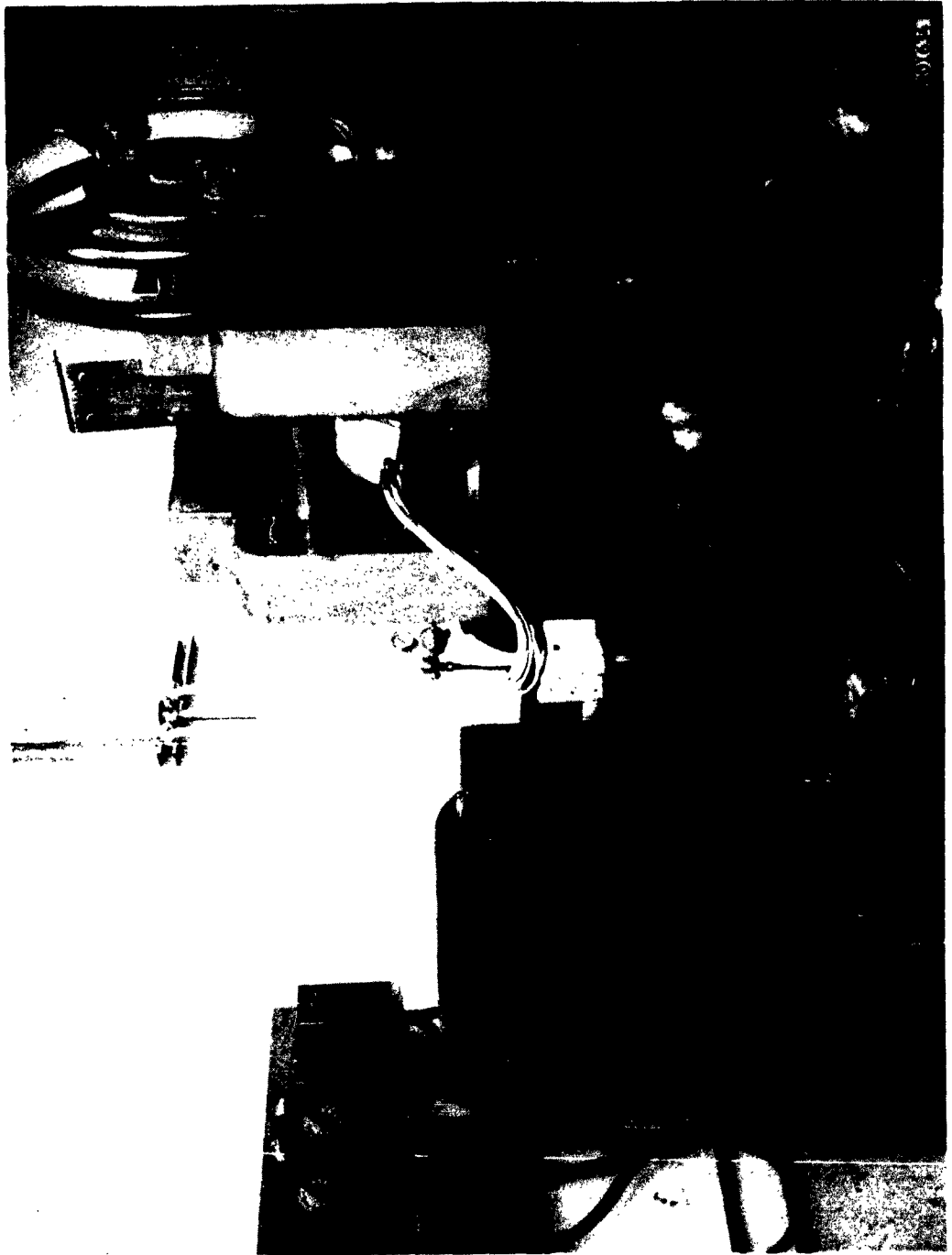
FIGURE 1. LOMA 600 ROLLING MILL MODIFIED FOR HIGH TEMPERATURE OPERATION.

FIGURE 2. TUBULAR FURNACE AND CONTROL UNITS FOR PRE-HEATING THE SAMPLE PRIOR TO ROLLING.

-10-

FIGURE 3.   84   PERCENT
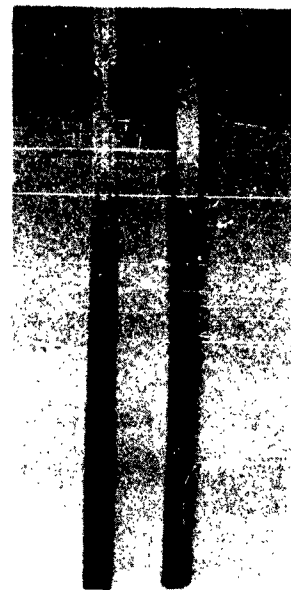
FIGURE 4.   47   PERCENT

FIGURE 5. 68   PERCENT

FIGURE 6. 81   PERCENT

R01636

CRYSTAL ORIENTATION (001) [100] AFTER VARIOUS AMOUNTS
OF DEFORMATION.   TOP OF FIGURE IS LEAD-END.

-11-

FIGURE 7. 42 PERCENT

FIGURE 8. 68 PERCENT

R01637

CRYSTAL ORIENTATION (011) [100] AFTER VARIOUS AMOUNTS OF
DEFORMATION.TOP OF FIGURE IS LEAD-END.
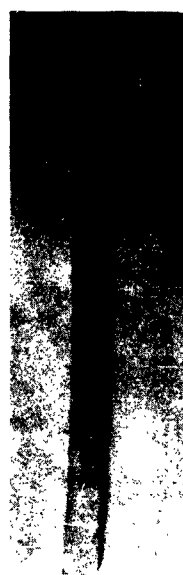
FIGURE 9. CRYSTAL ORIENTATION (001) [110] , 68 PERCENT REDUCTION IN TWO PASSES. TOP OF FIGURE IS LEAD-END,.3X.

FIGURE 10. CRYSTAL ORIENTATION (001) [110] , 87 PERCENT REDUCTION. NOTE CRACKING AT LEAD-END.

RO1638
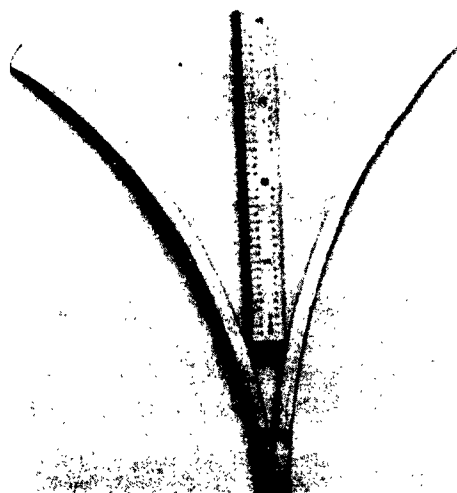
FIGURE 11.   47   PERCENT
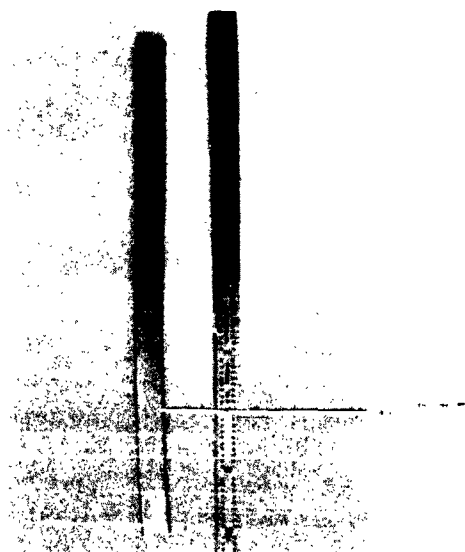
FIGURE 12.   42   PERCENT
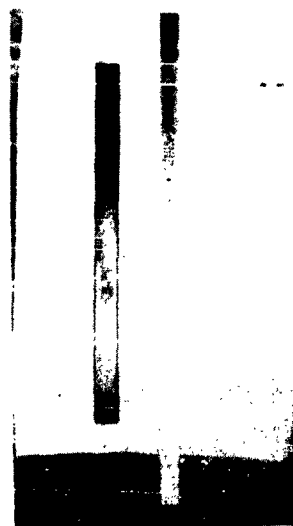
FIGURE 13.   68   PERCENT

CRYSTAL ORIENTATION (0$\bar{1}$1) [011] OF VARIOUS AMOUNTS OF DEFORMATION.
TOP OF FIGURE IS LEAD-END.

R01639

-14-

PART II

SECTION II-1

INTRODUCTION

        The purpose of the second phase of this program was to study
the possibility of annealing out substantial amounts of cold work intro-
duced into a single crystal during rolling without causing recrystalliza-
tion and associated embrittlement. Preliminary work was concerned with
the influence of such factors as crystal orientation, amount of deforma-
tion and types of substructure on the kinetics of recrystallization. The
substructure was identified with an etch pit technique which decorated
dislocations at the crystal surface. These results led to a method of
consecutive roll-anneals which supplied substantial amounts of deforma-
tion without recrystallization.

SECTION II-2

BACKGROUND

Recent interest in the properties of high-purity tungsten
has led several investigators to study electron beam zone-melted tungsten.
Almost invariably, the result of this method of purification is a single
crystal wire of small diameter. Such wires have been severely deformed
and subsequently annealed in hopes of obtaining high-purity polycrystalline
tungsten for comparison with tungsten of ordinary purity. However, it
has been very difficult to recrystallize the deformed single crystals,
in accord with the results described by Smithells.[1]

Under appropriate conditions, single crystals of tungsten were
cold-worked and subsequently softened by annealing without becoming poly-
crystalline. The procedure was repeated a number of times, still retaining
monocrystallinity, provided that the reduction in area between anneals
is not excessive. As much as 50 per cent reduction in area was tolerated
for wires about 2 mm in diameter.

There is some question as to whether large single crystals will
behave in the same manner as small diameter crystals. According to
Smithells, during drawing of large single crystals, even the smallest
reductions apparently exceeded a critical value, and recrystallization
occurred. However, there seems to be no *a priori* reason why large single
crystals should not behave in the same way as small ones, provided that
the proper conditions are maintained. It is expected that the type,
amount, and temperature of deformation, sample orientation, and geometry
will be important factors to be considered.

The observations described above, indicating that under certain
conditions recrystallization may be avoided in severely deformed tungsten
may be very significant for the following reasons:

-16-

(1) Rolled single crystal sheet material should be superior to polycrystalline tungsten simply because of the absence of high angle grain boundaries. Low-temperature ductility should be improved by eliminating the embrittling effect of the grain boundaries; creep resistance should be enhanced by eliminating grain boundary sliding; and preferential formation of oxides at the grain boundaries would not occur. The influence of the residual substructure after consecutive roll-anneals cannot be anticipated but a finer subgrain structure should further improve creep resistance.

(2) There is good reason to believe that the crystal growing method presently used by the Linde Company can be scaled up to permit casting of large, special shaped ingots, such as slabs for subsequent sheet rolling.

It is the purpose of this investigation to study the deformation and recrystallization behavior of tungsten single crystals of four different orientations in order to determine the conditions under which tungsten single crystals may be deformed by rolling, and subsequently annealed, without recrystallization.

SECTION II-3

EXPERIMENTAL PROCEDURE

II-3.1 MATERIAL

Tungsten single crystals, supplied by the Linde Company, were obtained in duplicate with the numerical designation and rolling orientation shown in Table II. The size of the single crystals was $\frac{1}{2}$ x $\frac{1}{4}$ x 6 inches with the method of deformation identical to that described in Part I. The temperature of all tungsten crystals prior to rolling was $1800^{\circ}F$ ($982^{\circ}C$) with a $\frac{1}{2}$ hour soak time. The rolls were kept at a temperature between $700-850^{\circ}F$ ($370-455^{\circ}C$).

II-3.2 ANNEALING PROCEDURE

The procedure for annealing during the recrystallization study was established with a $1\frac{1}{2}$ inch long sample from a (001) [110] crystal. The sample was rolled 60 per cent in one pass at $1800^{\circ}F$ ($982^{\circ}C$). The general features of the as-rolled structure are illustrated in Figure 14. Annealing for $\frac{1}{2}$ hour in vacuum at $1500^{\circ}C$ resulted in recrystallization as typified in Figure 15. Good temperature control and the absence of oxide formation during annealing was obtained. The $\frac{1}{2}$ hour annealing time was satisfactory and, unless otherwise specified, was used for all samples.

A series of four samples were cut off the crystal after each deformation. Three samples were annealed at different temperatures in order to bracket the recrystallization temperature. The one remaining as-rolled sample was used as a back-up in case it was necessary to duplicate results or more closely define the recrystallization temperature. Samples used in the recrystallization study were approximately $\frac{1}{4}$ x $\frac{1}{2}$ inch square. The vacuum furnace operated at 10^{-4} mm of Hg. A brightness temperature of the sample was recorded using a micro-optical pyrometer with an accuracy of $\pm25^{\circ}C$. The brightness temperature was then converted to true temperature.

-18-

TABLE II

NUMERICAL DESIGNATION OF DIFFERENT CRYSTAL ORIENTATIONS

1616-74	1616-73	1616-12	1616-34
(001) [$\bar{1}$00]	(011) [100]	(001) [110]	(1$\bar{1}$0) [110]

1616-16	1616-38	1690-9	1616-57
(001) [100]	(011) [100]	(100) [011]	(0$\bar{1}$1) [011]

1690-12

(100) [011]

II-3.3 ETCH PIT TECHNIQUE

An etchant, suggested by Hull and Anderson,[2] was used for electrolytic polishing and etching of the tungsten single crystals. The reagent was 160 gm of Trisodium Phosphate mixed with 1000 ml H_2O. The solution was maintained between 100-120°F with a current density of .09/A cm^2.

Etch pits were obtained which revealed the emergence of dislocations at the surface of the crystal in the same way as the etch pits obtained with the reagent used by U. E. Wolff[3] and further studied by H. W. Schadler.[4] Square pits are found on the $\{100\}$, Figure 16, triangular pits on the $\{111\}$, Figure 17, and pits which appear as elongated droplets, Figure 18, on the $\{112\}$. The $\{110\}$ are not attacked by the reagent. The density of the pits is found independent of time but this variable strongly influences the size. Longer times produce larger pits. The dislocation density of the as-received crystals was estimated using etch pits to be about 5 x 10^5 on the $\{100\}$. The shape of the pits can also be used to estimate the orientation of new grains formed during recrystallization.

In establishing the technique for electrolytic polishing and etching with trisodium phosphate, an experiment was performed which also illustrates the usefulness of the etch pit technique. Since some interesting results were obtained which demonstrate the behavior of b.c.c. single crystal tungsten in compression at room temperature, the experiment will now be discussed in some detail.

A cube shaped $\{010\}$ type single crystal was polished, etched (Figure 19) and subsequently deformed in uniaxial compression at room temperature. The square pits in Figure 19, identify the $\{010\}$, and also provide an estimate of the original dislocation density. After a 0.1 per cent deformation, the crystal was re-etched and the area, first observed, relocated. The result is shown in Figure 20, where the smaller pits identify the emergence of new dislocations or the relocation of some of the existing dislocations. The pits presented in Figure 19 existed prior to deformation and now have been enlarged. Gilman and Johnson[5] have done similar work on LiF.

A uniform dislocation multiplication appears throughout the volume of the crystal. The surface is identified as a dislocation source by the large concentration of etch pits at the edge. If a similar effect results from rolling, it would be advisable to polish between rolling passes to eliminate the regions of high localized deformation. Repolishing the same area, Figure 21, removes all history of dislocation sites and

subsequent etching reveals only the existing dislocations. The boundary which existed in the as-received crystal, on the left side of the observed area in Figure 19 has disappeared, Figure 21, indicating that the subgrain boundaries present in the as-received crystal are unstable at room temperature and easily destroyed by stress alone. Koo[6] suggests that subgrain boundaries behave in much the same way as grain boundaries in acting as barriers for dislocations pile-ups since an analysis of yield strength versus grain size according to the Petch equation, gives numbers which appear to be reasonable. Photographic evidence was obtained in this investigation which definitely illustrates the instability of the subgrain boundaries present in the as-received crystals. In fact, it will be shown that a 10 per cent reduction by rolling at 1800°F is adequate to destroy existing subboundaries in the as-received material with the resulting formation of finer subgrains. It is conceivable, however, that the finer subgrains might be of a different type and behave in the fashion described by Koo.

The etch-pit technique was used throughout this investigation since the etch pits reveal the behavior of dislocations at the surface of a single crystal of tungsten at low deformations and permit an estimate of the orientation of crystallites formed during annealing. Foils for electron transmission microscopy studies of substructure were successfully prepared using the trisodium phosphate reagent but the time consumed in foil preparation and the necessity for observing the over-all substructural behavior during deformation and subsequent annealing, made the technique undesirable. Specific areas of investigation for future transmission studies are suggested as a result of the etch pit observations.

SECTION II-4

RESULTS

        The recrystallization temperature was defined as the tempera-
ture at which crystallites first appear after a ½ hour anneal. Four
different orientations were used in determining this recrystallization
as a function of deformation. Figure 23 illustrates the recrystalli-
zation temperature for reductions of less than 50 percent for each
orientation. It can be seen that beyond 30 per cent reduction all the
orientations show crystallites first appearing at nearly the same tem-
perature, with the exception of the (1T0) [110] orientation.

        The influence of orientation on the appearance of the first
crystallites is most significant at reductions less than 30 per cent.
The (100) [011] displays no recrystallization at 2500°C after 5 per
cent deformation. The results of the (100) [011] orientation appear
most promising for consecutive roll-anneals without recrystallization
although the (011) [100] possibly behaves in a similar fashion.

II-4.1 DEFORMATION BEHAVIOR OF VARIOUS ORIENTATIONS

        The gross deformation behavior of the (100) [011] and the
(011) [100] crystals was similar with large amounts of deformation
causing a banded structure to appear on the rolling plane. The deforma-
tion bands were perpendicular to the rolling direction. Edge effects
are apparent which suggest a mode of deformation different from that of
the bulk material since the slip traces are of different orientation
from those in the bulk material (Figure 22).

        Only the (100) [011] crystal was observed at the early stages
of deformation since the (011) is not attacked by the reagent. Subgrains

-22-

2-3 mm in diameter (Figure 24) were apparent in the as-received
crystal. After 3.3 per cent deformation the subgrain boundaries
were almost completely annihilated (Figure 25) and the dislocation
density had increased in a random fashion. At 5.0 per cent deforma-
tion (Figure 26), the dislocation density had further increased,
giving the appearance of a cellular structure 30 μ in diameter. The
dislocation density was about 5 x 10^7. At 9.8 per cent deformation,
striations formed of an agglomeration of etch pits, begin to appear
(Figure 27). The process continues until a banded structure forms
(Figures 28 to 30). The deformation bands are alternate layers of
(100) and (112) etch pits with the bands in the [0ī1] direction.
The banded structures can be observed microscopically in Figures 29
and 30 and macroscopically in Figure 22. Edge effects due to rolling
are evident.

Assuming that slip occurs on the {110} or {112}, there are
only two planes which can account for the slip traces. The operative
slip systems are the (2ī1) [ī11] and the (2ī1) [111]. The maximum
resolved shear stress acts on these planes if the applied stress is
assumed to be compressive in the [ī00]. Since in actuality, rolling
stresses deviate from pure compression, it is quite possible that only
one slip system is operative, especially during the early stages of
deformation. Increased deformation would be expected to cause lattice
rotation and consequently introduce other slip systems. A similar
argument should hold for the (011) [100] crystal in accord with the
observed deformation bands (Figure 31).

The gross deformation behavior of the remaining two orienta-
tions were also similar to each other with both the (001) [100] and the
(1ī0) [110] showing cross-hatched {110} slip traces after large amounts
of deformation (Figure 32). Edge effects due to rolling are also
apparent. The (001) [100] , which is subject to etch pit analysis,
also displays an increase in the dislocation density at the expense of
the existing sub-boundaries with deformation. Figure 33 shows a dis-
persion of etch pits which appear to form cellular structures of about
30-50 μ after 7.5 per cent deformation.

II-4.2   RECRYSTALLIZATION BEHAVIOR OF VARIOUS ORIENTATIONS

The (100) [011] crystal was deformed 3.3, 5.0, 15.7. 16.0,
22.5 and 43.4 per cent prior to annealing. The data points indicating
the onset of recrystallization, defined as the temperature at which
crystallites first appear after a ½ hour anneal, are given in Figure 34.

-23-

The new grains first begin to appear within the deformation bands at the edge of the crystal. Higher temperatures were needed to cause recrystallization in the bulk material. No signs of recrystallization were obtained on annealing at 2500°C after 5 per cent deformation.

The (011) [100] crystal which possesses similar gross deformation characteristics, displays similar recrystallization characteristics. Deformations of 3.9, 5.9, 18.1 and 43.7 per cent were used prior to annealing. New crystallites again first appeared at the edges as shown in Figure 31, with the data points indicating the onset of recrystallization plotted in Figure 35. The recrystallization temperature at 20 per cent deformation was found to be 100°C higher in the (011) [100] than in the (100) [011] crystal. At 5 per cent deformation the (011) [100] orientation showed no recrystallization at 1800°C, the highest annealing temperature used for this crystal. Thus, the possibility of favorable recrystallization characteristics for this crystal also exists.

The two crystals which had cross-hatched slip traces present after rolling possessed the least favorable recrystallization characteristics. The (001) [100] crystal was deformed 5.5, 7.5, 20.9 and 44.6 per cent prior to annealing. New grains first appeared within the deformation bands at the edges (Figure 36). The maximum recrystallization temperature for this crystal was 1800°C after 5 per cent reduction with the remaining values plotted in Figure 38.

The (1$\bar{1}$0) [110] was deformed 1.0, 3.2, 6.4, 23.2 and 53.0 per cent prior to annealing. From the recrystallization data points plotted on Figure 39, it is apparent that there is no reasonable amount of deformation below which recrystallization will not occur. The crystallites appear at random at 1200°C for 53 per cent deformation (Figure 37).

If the curves which best fit the data points are compared, the influence of increasing deformation on the first appearance of crystallites for four different orientations is illustrated (Figure 23). The difference in temperature at which these crystallites first appear in the four orientations at a given reduction is most significant at less than 30 per cent. Beyond 30 per cent the differences diminsh.

-24-

II-4.3 ORIENTATION OF FIRST FORMED CRYSTALLITES

All four orientations produced recrystallized grains of the {100} which is common for polycrystalline b.c.c. materials. This particular orientation was in the majority except for the (001) [100] crystal, which possessed a majority of (112) crystallites and a minority of (100). The recrystallized grains appear with an orientation either identical to the matrix, recrystallization *in-situ*, shown in Figure 40, or with an orientation different from the matrix (Figure 41). The first type of crystallite formation very likely results from poly-gonization and subgrain boundary migration at the expense of annihilating existing dislocations. Figure 40 illustrates this behavior by comparing the low dislocation density within the grain to the dislocation density of the matrix.

II-4.4 CONSECUTIVE ROLL-ANNEALS

The (001) [110] crystal was chosen for this portion of the investigation based on the results of no recrystallization after 5 per cent reduction and a 2500°C anneal.

Other observations in the recrystallization temperature studies suggested the following procedures and precautions be taken in attempting to acquire a large amount of deformation by consecutive roll-anneals and still maintain the monocrystallinity of the crystal.

(a) Anneal the as-received crystals at the highest possible temperature to reduce the dislocation density, for the dislocation density appears to be strongly temperature dependent. Assuming the dislocation density plays a significant roll in the recrystallization behavior, a minimum density at the beginning of deformation would consequently be preferred. A comparison of Figures 42 and 43 illustrates the decrease in dislocation density due to annealing prior to working.

(b) Any irregularities such as burrs which might cause high local distortions should be removed. As an extra precaution, all specimens were electrolytically polished prior to rolling, and also between passes, in order to eliminate edge effects in the crystal.

-25-

(c) The deformation per pass should be less than
5 per cent.

(d) After rolling, any oxide film should be removed
either by mechanical or chemical means.

(e) Annealing should be done at the highest possible
temperature in order to minimize the time for
recovery and also minimize the number of remaining
dislocations. The considerable difference in the
dislocation density as a function of temperature
is illustrated by comparing duplicate specimens
annealed at different temperatures as illustrated
in Figures 44 and 45.

With the above procedures and precautions, three roll-anneals
were successfully completed with no recrystallization occurring after
annealing a specimen at 2500°C with a total of 9.4 per cent deformation
due to rolling. For another sample of the same crystal orientation,
recrystallization was observed at 1700°C for the same amount of deforma-
tion, without intermediate annealing. It therefore seems possible that
consecutive roll-anneals can be used to produce single crystal sheet.

The results of the work on the consecutive roll-anneals will
now be discussed in detail. A (001) [110] crystal, 1.5 inch long and
0.251 inch thick was electropolished to 0.246 inch. A one-half hour,
2500°C anneal was used to minimize the dislocation density. The thick-
ness was then reduced to 0.237 (3.7%) by rolling. Electropolishing to
0.233 inch and etching reveal a new dislocation pattern (Figure 46). An
increase in dislocation density is detected. Annealing one half hour
at 2500°C, electropolishing to 0.226 inch, and etching produce a decrease
in dislocation density (Figure 47). Another 4 per cent reduction (0.217
inch), polish, and etch, produce the high etch pit density illustrated
in Figure 48. Annealing one half hour at 2500°C, electropolishing to
0.209 inch, and etching, supplies another low density substructure
(Figure 49). A total of 7.4 per cent reduction has been obtained with
no evidence of crystallites forming after a 2500°C anneal.

The crystal was repolished to 0.207 inch and rolled a third
time to a total of 9.4 per cent reduction (.202 inch thick, Figure 50).
Polishing to 0.198 inch and etching, illustrates the existing high dis-
location density. Again annealing for one half hour at 2500°F produces
a very low dislocation density (Figure 51) which is still quite similar
to the density of the annealed, as-received crystal. There is still no
evidence of crystallites forming after a total of 9.4 per cent reduction.

-26-

SECTION II-5

DISCUSSION

In order to discuss the results of this investigation, it would be of value to refer to the work of Nakayama, Weissman and Imura[7] where three substructural entities are identified in cold worked tungsten single crystals. They are:

(a) Macroscopic substructure (1st order subgrains), 2-8 mm

(b) Microscopic substructure (2nd order subgrains), $30-50\mu$

(c) Third order subgrains, $5-10\mu$

With the reference to this nomenclature, the substructure resulting from rolling tungsten single crystal at $982°C$ ($1800°F$) can be discussed as follows:

(a) First order subgrains present in the as-received single crystals are destroyed with very small amounts of deformation. This effect is even true at room temperature as evidenced by 0.1 per cent compressive strain being sufficient to cause annihilation of some of the subgrain boundaries.

(b) The resistance of the first order subgrain boundaries to annihilation appears to be strongly dependent on the disorientation angle across the boundary. The behavior is such that increasing amounts of deformation are necessary to annihilate subgrain boundaries of increasing disorientation angle.

-27-

(c) As the first order subgrains are being eliminated,
     the dislocation density increases and etch pits
     are observed which take the form of a cellular net-
     work with an average diameter of about 30μ, i.e.,
     second order subgrains.

(d) Etch pits begin to form striated agglomerates at
     deformation beyond 10 per cent. The striations,
     which are the first appearance of slip traces,
     have a minimum initial spacing similar to the
     diameter of the second order subgrains. At deforma-
     tions beyond 10 per cent, transmission electron
     microscopy has shown[7] the formation of third order
     subgrains. Since the etch pit technique does not
     have sufficient resolution to identify the third
     order subgrains, it has been assumed that the striated
     agglomerates are the regions where third order sub-
     grains first appear. In general, the first order
     subgrains have been annihilated at the onset of the
     deformation of third order subgrains.

There was no influence of orientation on the development of
the etch pattern with deformation for the (001) [100] and (100) [011]
crystals. At low deformations where the substructures appeared to be
identical, each crystal responded differently to annealing. The (100)
[001] recrystallized at 1800°C after 5 per cent deformation whereas the
(100) [011] did not recrystallize for the same amount of deformation
even at 2500°C. A difference in substructure must therefore exist which
is not reflected in etch pit analysis.

One fact which might explain this behavior is the appearance
of cross hatched slip traces in the (100) [001] crystal and parallel
slip traces in the (100) [011] crystal at larger deformations. These
slip traces suggest that multiple slip is taking place in the (100)
[001] crystal even at small deformation. Such slip results in complex
subgrain or subcell boundaries due to intersection. On the same basis,
simple slip is taking place in the (100) [011] crystal at small deforma-
tion and a simple type of boundary results. Obtaining etch pit patterns
on the surface of the crystal would not necessarily reveal the
complexity of these subgrain boundaries.

The existence of a more complex boundary under multiple
slip, which is not revealed by etch pit analysis, might explain the
observations of Semmel and Machlin [8] in single crystals of silver. A
low temperature anneal was found to increase the recrystallization

-28-

temperature of a crystal deformed under conditions of multiple slip, without a significant change in dislocation density. A rearrangement of dislocations within the subgrain boundaries might have resulted with no significant change in the dislocation density as revealed by etch pits. The boundaries might have changed from a complex to a simple type with no indication from etch pit analysis, and consequently be governed by different laws of migration. The thermal energy for boundary migration should vary not only with the disorientation angle across the boundary, which is a function of dislocation density, but also the type of boundary which is not revealed by etch pit analysis.

The fact that different boundaries are formed when deformation is obtained by simple or multiple slip was shown by Vogel.[9] A homogeneous aggregation of dislocations produced when only one slip system was operative, lent itself to polygonization; whereas, when intersecting sets of dislocations were produced, polygonization did not readily occur. These observations support the concept of more complex subgrain boundaries forming under conditions of multiple slip than under conditions of simple slip with the over-all etch pit pattern in each case being similar. Thus a different recrystallization behavior of the crystals with different orientations and similar etch pit patterns could result.

In order to obtain complete recovery without recrystallization, a crystal must be chosen with an orientation such that rolling stresses will be accompanied by deformation on one slip system. Small amounts of deformation per pass must also be used in order to limit the possibility of other slip systems becoming operative which would result in a condition of multiple slip. Also, large amounts of deformation might form subgrains with large amounts of disorientation relative to the matrix since dislocations have been shown to move into subgrain boundaries with increasing deformation. As a result, the disorientation angle increases. As the orientation of the subgrain relative to the matrix changes, the probability of crystallites of different orientation than the matrix forming, also increases. The reason is based on the work of Jones,[10] for example, who has shown in his work on the recovery of tungsten, that subgrains formed during deformation eventually form grains on annealing.

Therefore, if the necessary precautions are taken, resulting cells would have very little disorientation relative to the matrix and their subgrain boundaries would be of a simple type, tilt boundaries for example. Annealing would cause polygonization, subsequent boundary migration and eventually, complete recovery without a change in crystal orientation, i.e., recrystallization _in situ_. These observations were

-29-

verified by the results on the consecutive roll-anneals where 9.4 per cent total deformation was obtained with no recrystallization evident at 2500°C, and the final dislocation density was similar to the annealed as-received crystals.

SECTION II-6

SUMMARY

1. Experimentally the crystal orientation most favorable to
    recovery without recrystallization after deformation by rolling
    at 982°C is the (001) [110] which is the recrystallization tex-
    ture for polycrystalline tungsten. Another possibility which
    was not explored to completion was the (110) [001] .

2. Considering the slip systems available and the type of stresses
    encountered in rolling, the initial stages of deformation for the
    (001) [110] and (110) [001] crystals can be expected to occur by
    slip on one system.

3. The first stages of deformation cause annihilation of first order
    subgrains (2-8 mm) and formation of second order subgrains (30-50 μ).

4. Regions of high localized deformation generally appear at the
    rolling surfaces and edges of the crystal and consequently can be
    removed with adequate polishing between rolling passes.

5. If the crystal is not polished after deformation, crystallites
    first appear in regions of high local deformation, normally at the
    edges.

6. Recrystallized grains can appear both with their orientation
    greatly different from the matrix or identical to the matrix.

7. Although etch pit patterns of cell formation are similar in both
    cases, slip on one system produces sub-boundaries of a simple type
    conducive to complete recovery without recrystallization; whereas,
    multiple slip lends itself to the formation of complex subgrain
    boundaries which lend themselves to recrystallization.

-31-

8. Consecutive roll-anneals with properly oriented crystals are a successful way of obtaining large amounts of deformation in single crystals with no apparent recrystallization to temperatures of $2500^{\circ}C$.

REFERENCES

1. C. J. Smithells, <u>Tungsten</u>, Chemical Publishing Co., Inc., p. 150, 1953.

2. F. C. Hull and R. L. Anderson, Scientific Paper 6-94402-11-P2, Westinghouse Research Lab., Pittsburgh, Pa.

3. U. E. Wolff, <u>Acta Met.</u>, 6, 559 (1958).

4. H. W. Schadler, "Direct Observations of Imperfections in Crystals," AIMMPE Conference, March 1961, p. 593.

5. J. J. Gilman and W. G. Johnston, <u>J.A.P.</u>, 30, No. 2, 129 (1959).

6. R. C. Koo, <u>J. of Less Common Metals</u>, 3, 412 (1961).

7. Y. Nakayama, S. Weissmann and T. Imura, "Direct Observations of Imperfections in Crystals, AIMMPE Conference, March, 1961, p. 573.

8. J. W. Semmel, Jr. and E. S. Macklin, <u>Acta Met.</u>, 5, 582 (October 1957).

9. F. L. Vogel, Jr., <u>Acta Met.</u>, 6, 532 (1958).

10. F. O. Jones, <u>J. Less Common Metals</u>, 3, 163 (1960).

FIGURE 14. CRYSTAL (001) [110] DEFORMED 60 PERCENT IN ONE PASS. 16X

FIGURE 15. CRYSTAL (001) [110] DEFORMED 60 PERCENT REDUCTION OF
THICKNESS IN ONE PASS. ANNEALED 1500°C FOR 1/2 HOUR.
120X

-35-

FIGURE 16. SQUARE ETCH PITS ON THE {100} SURFACES. 400X

FIGURE 17. TRIANGULAR ETCH PITS ON THE {111} SURFACE. 12,000X
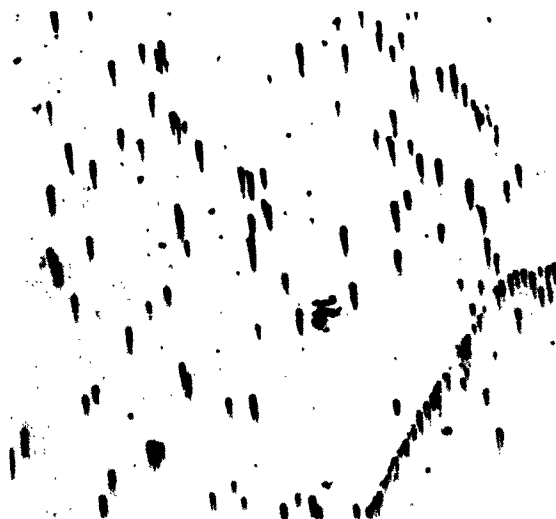
FIGURE 18. DROPLET SHAPED PITS ON THE {112} SURFACE. 500X

-36-

FIGURE 19. SELECTED AREA NEAR EDGE OF ANNEALED CRYSTAL TO BE
            SUBJECT TO ROOM TEMPERATURE COMPRESSION. 400X
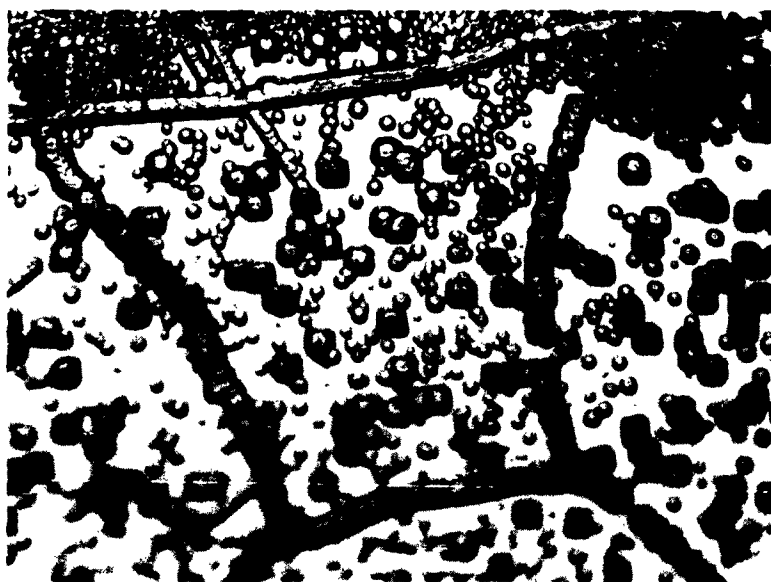
FIGURE 20. SAME AREA AS FIGURE 19 AFTER 0.1 PERCENT R.T. COMPRESSIVE STRAIN AND
            RE-ETCH. NOTE LARGE DENSITY OF PITS AT THE STRESSED SURFACE. 400X
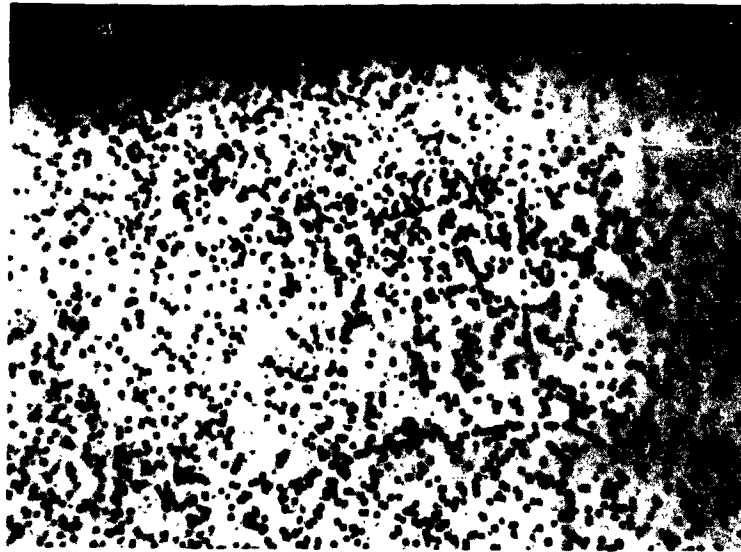
R01643

FIGURE 21. SAME AREA AS FIGURE 20 AFTER REPOLISH AND ETCH.
NOTE SUBBOUNDARY ON LEFT HAS BEEN ANNIHILATED. 400X

FIGURE 22. CRYSTAL ORIENTATION (100) [011] DEFORMED 43.4 PERCENT.
NOTE BANDED STRUCTURE. 7.5X

RO1644

-38-
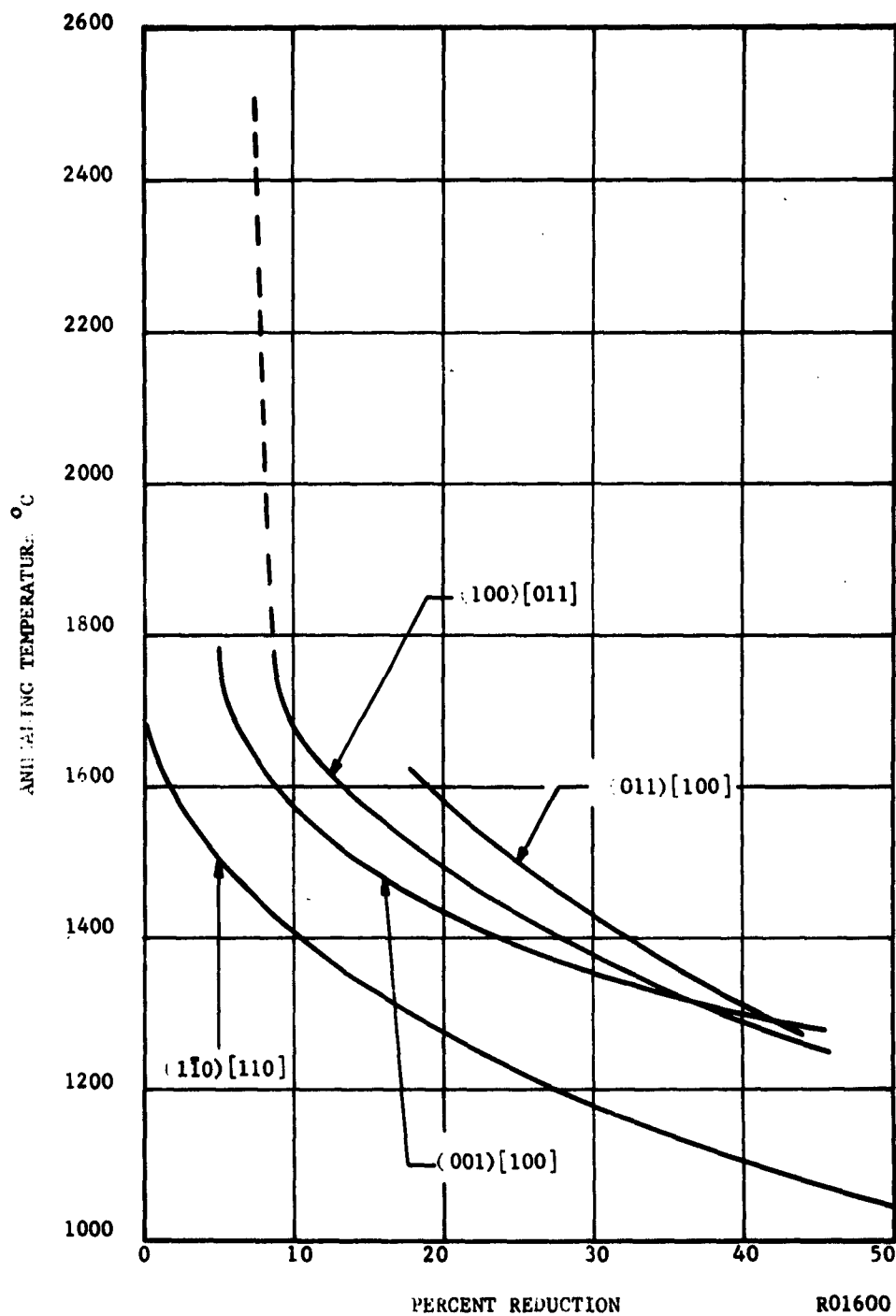
FIGURE 23. EFFECT OF DEFORMATION ON THE RECRYSTALLIZATION TEMPERATURE OF FOUR DIFFERENT CRYSTAL ORIENTATIONS.

-39-

FIGURE 24. AS-RECEIVED CRYSTAL OF ORIENTATION (100) [011] . 100X

FIGURE 25. CRYSTAL IN FIGURE 24 AFTER 3.3 PERCENT REDUCTION. NOTE BOUNDARIES
ARE ANNIHILATED AND CELLULAR APPEARANCE OF PITS RESULTS. 100X

R01645

-40-

FIGURE 27. 9.8 PERCENT
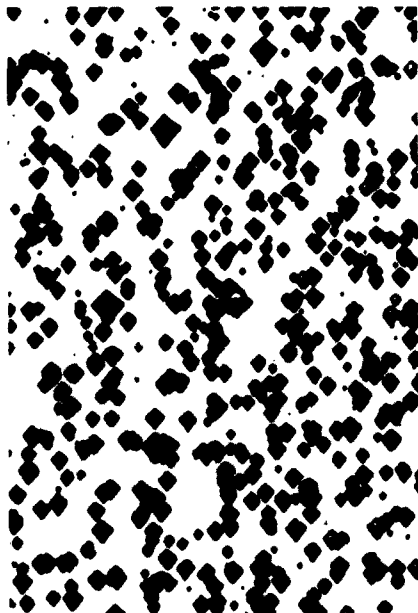
FIGURE 26. 5 PERCENT

FIGURE 28. 16 PERCENT

R01646

PROGRESSIVE DEVELOPMENT OF SUBSTRUCTURE WITH
DEFORMATION FOR CRYSTAL SHOWN IN FIGURE 24. 500X
NOTE SEQUENTIAL DEVELOPMENT OF INCREASING DENSITY,
CELLULOR CONFIGURATION AND STRIATED AGGLOMERATES.

-41-

FIGURE 29. CRYSTAL (100) [011] OF FIGURE 24 AFTER 22.5 PERCENT REDUCTION. NOTE FIRST APPEARANCE OF DEFORMATION BANDS. 500X

FIGURE 30. AFTER 43.4 PERCENT, BANDED STRUCTURE IS READILY APPARENT. ETCH PITS REVEAL DIFFERENCE IN ORIENTATION BETWEEN DEFORMATION BAND AND MATRIX. 500X

R01647
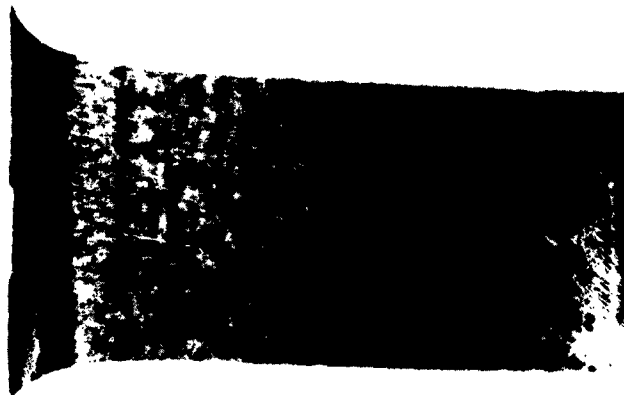
FIGURE 31. CRYSTAL (011) [100], ANNEALED AT 1400°C FOR 0.5 HOUR AFTER 43.7 PERCENT DEFORMATION. 7.5X
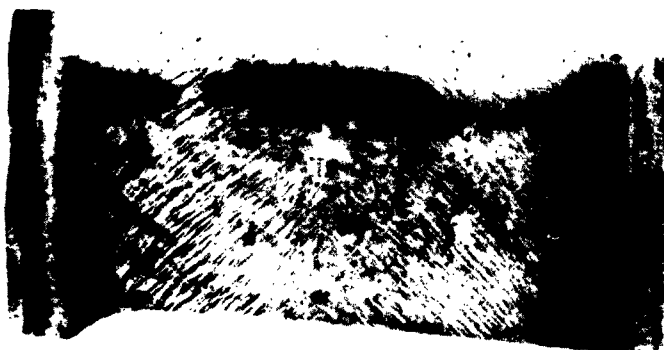
FIGURE 32. 44.5 PERCENT, 7.5X

FIGURE 33. 7.5 PERCENT, 500X

CRYSTAL (001) [100] ILLUSTRATING CROSS-HATCHED SLIP TRACES AT LARGE DEFORMATIONS AND CELLULAR DENSITY AT LOW DEFORMATIONS

R01648
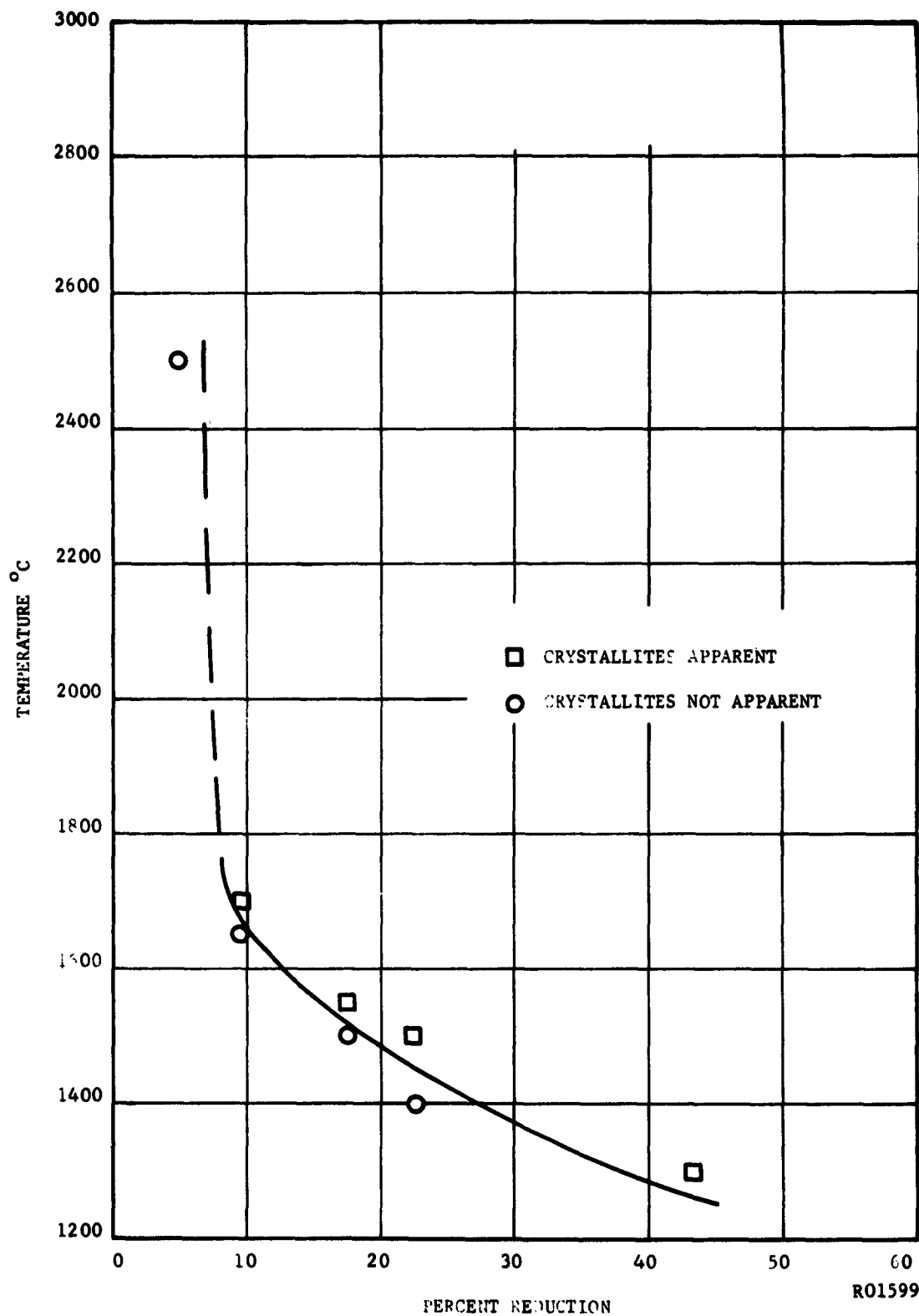
FIGURE 34. THE EFFECT OF DEFORMATION ON THE RECRYSTALLIZATION
TEMPERATURE OF THE (100) [011].

-44-
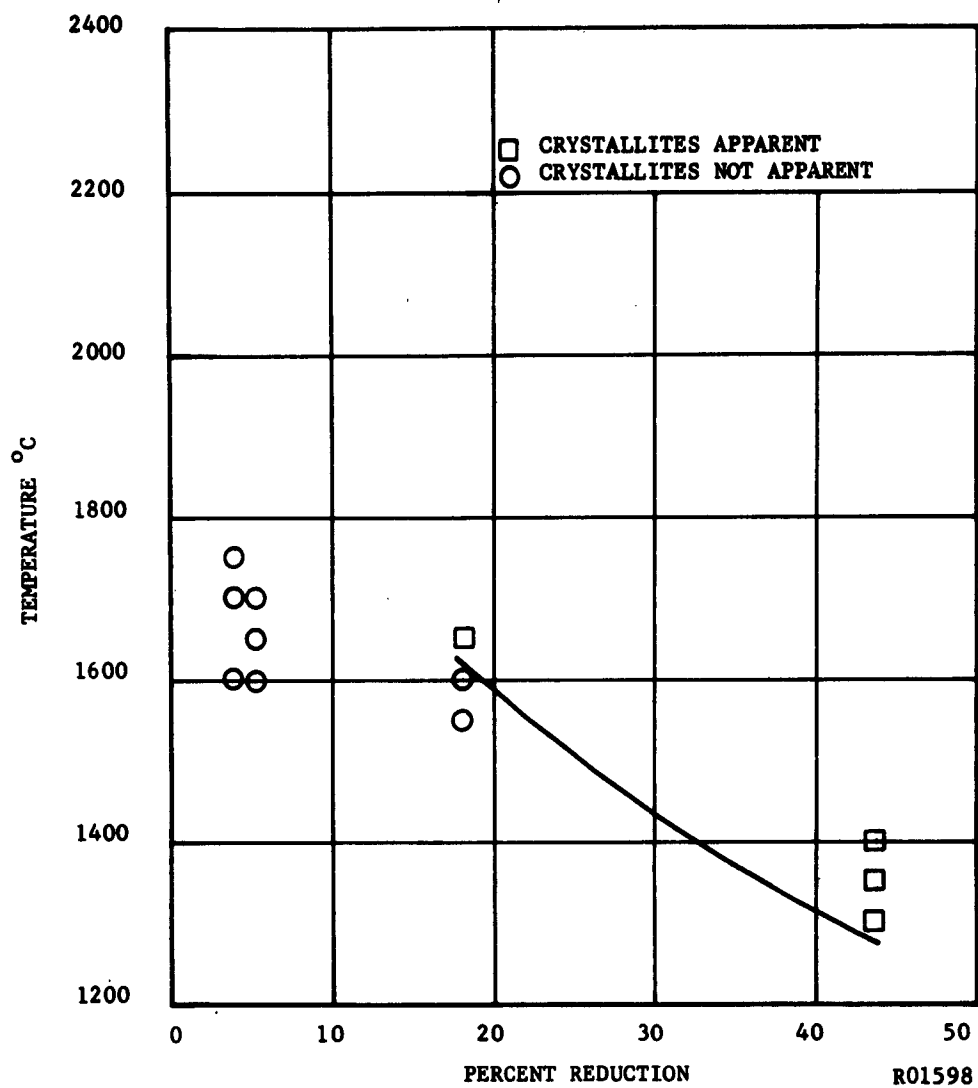
FIGURE 35. THE EFFECT OF DEFORMATION ON THE
RECRYSTALLIZATION TEMPERATURE OF
THE (011)[100]

-45-

FIGURE 36.   CRYSTAL ORIENTATION (001) [100] , ANNEALED AT 1400°C AFTER 44.6 PERCENT
DEFORMATION.   NOTE FIRST APPEARANCE OF CRYSTALLITES AT EDGES. 7.5X

FIGURE 37.   CRYSTAL ORIENTATION (1̄10) [110] , ANNEALED AT 1200°C
AFTER 53.0 PERCENT DEFORMATION. 7.5X

R01649

-46-
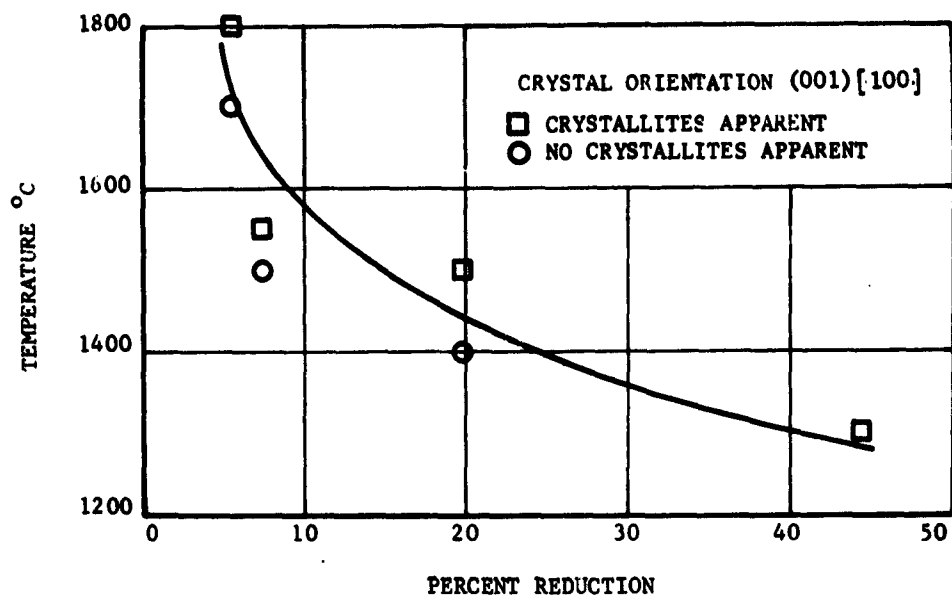
FIGURE 38. R_X TEMPERATURE FOR CRYSTAL (001) [100]
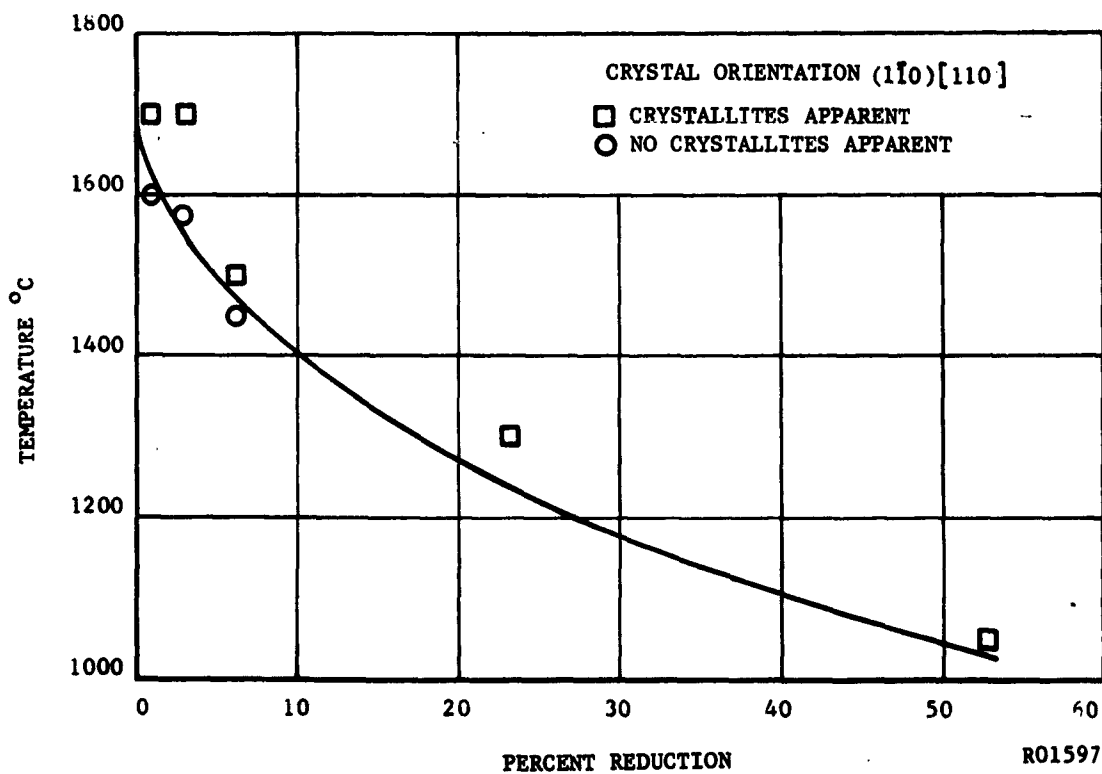
R01597

FIGURE 39   EFFECT OF DEFORMATION ON THE RECRYSTALLIZATION
TEMPERATURE FOR CRYSTAL (1$\bar{1}$0) [110].

-47-
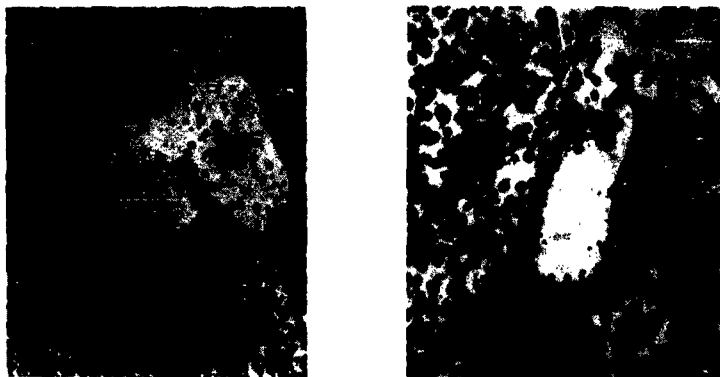
FIGURE 40. CRYSTAL (100) [011] ILLUSTRATING RECRYSTALLIZED GRAINS
OF ORIENTATION IDENTICAL TO MATRIX. 500X

FIGURE 41. CRYSTAL (1Ī0) [110], ETCH PITS IDENTIFY CRYSTALLITES
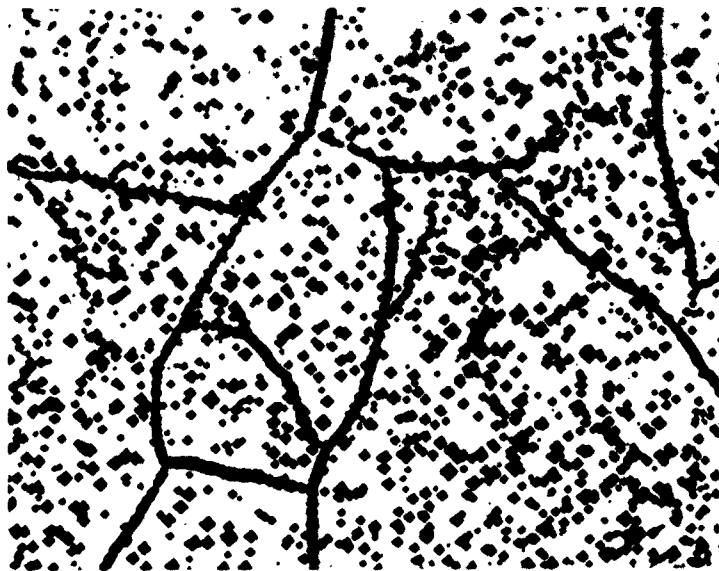OF DIFFERENT ORIENTATION THAN MATRIX. 500X

R01650

-48-

FIGURE 42. AS-RECEIVED CRYSTAL (100)[011]. 100X

FIGURE 43. ANNEALED, AS-RECEIVED CRYSTAL SHOWN IN FIGURE 42. TEMPERATURE OF ANNEAL WAS 2500°C. NOTE DECREASE IN ETCH PIT DENSITY. 100X
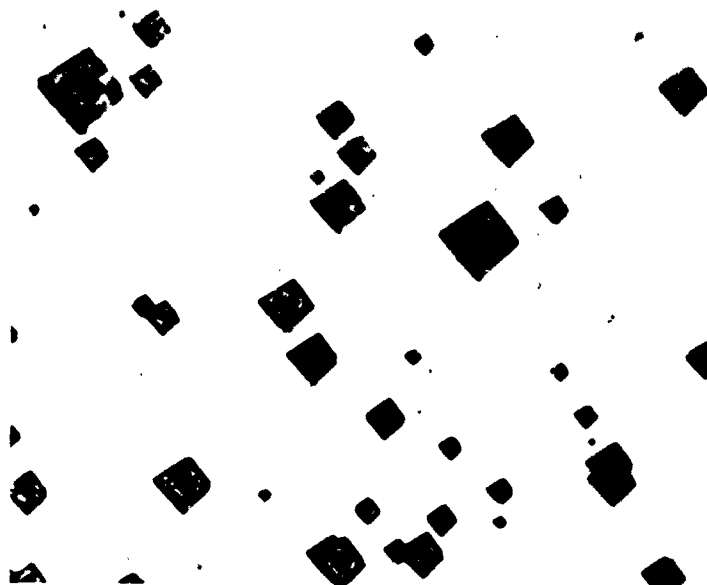
R01651

-49-

FIGURE 44. CRYSTAL (100) [011] ANNEALED AT 2500°C FOR 5 MINUTES
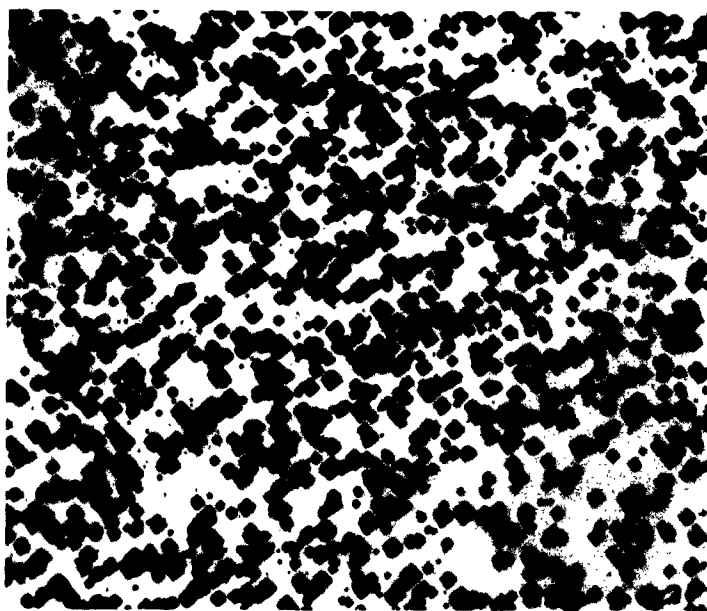AFTER 5 PERCENT REDUCTION. 500X

FIGURE 45. CRYSTAL (100) [011] ANNEALED AT 1850°C FOR 2 HOURS AFTER
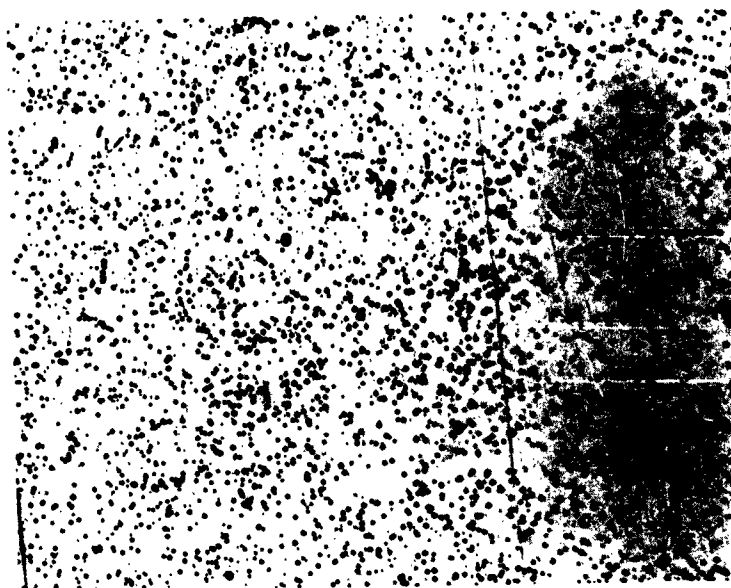5 PERCENT REDUCTION. 500X

R01652

FIGURE 46. CRYSTAL (100) [011] AFTER A 3.2 PERCENT REDUCTION. 100X

FIGURE 47. CRYSTAL OF FIGURE 46 ANNEALED AT 2500°C FOR 1/2-HOUR. 100X

R01653

FIGURE 48.   CRYSTAL OF FIGURE 47 DEFORMED A TOTAL OF 7 PERCENT AFTER A SECOND PASS. 100X

FIGURE 49.   CRYSTAL OF FIGURE 48 ANNEALED 1/2-HOUR AT 2500°C.
NOTE LOW ETCH PITCH DENSITY. 100X

R01654

FIGURE 50. CRYSTAL OF FIGURE 49 DEFORMED TO A TOTAL OF 9.4 PERCENT AFTER THIRD PASS. 100X
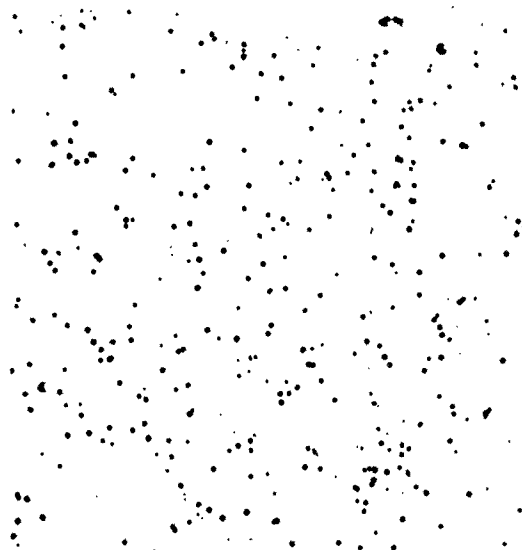

FIGURE 51. CRYSTAL OF FIGURE 50 ANNEALED AT 2500°C FOR 1/2-HOUR TO AGAIN REDUCE THE ETCH PIT DENSITY. 100X

R01655

-53-